


RESEARCH

Open Access



# DHCR24 reverses Alzheimer's disease-related pathology and cognitive impairment via increasing hippocampal cholesterol levels in 5xFAD mice

Wen-bin Zhang<sup>1†</sup>, Yue Huang<sup>1†</sup>, Xiao-rou Guo<sup>1</sup>, Meng-qi Zhang<sup>1</sup>, Xiang-shan Yuan<sup>1,2,3\*</sup> and Heng-bing Zu<sup>1\*</sup> 

## Abstract

Accumulating evidences reveal that cellular cholesterol deficiency could trigger the onset of Alzheimer's disease (AD). As a key regulator, 24-dehydrocholesterol reductase (DHCR24) controls cellular cholesterol homeostasis, which was found to be downregulated in AD vulnerable regions and involved in AD-related pathological activities. However, DHCR24 as a potential therapeutic target for AD remains to be identified. In present study, we demonstrated the role of DHCR24 in AD by employing delivery of adeno-associated virus carrying DHCR24 gene into the hippocampus of 5xFAD mice. Here, we found that 5xFAD mice had lower levels of cholesterol and DHCR24 expression, and the cholesterol loss was alleviated by DHCR24 overexpression. Surprisingly, the cognitive impairment of 5xFAD mice was significantly reversed after DHCR24-based gene therapy. Moreover, we revealed that DHCR24 knock-in successfully prevented or reversed AD-related pathology in 5xFAD mice, including amyloid- $\beta$  deposition, synaptic injuries, autophagy, reactive astrocytosis, microglial phagocytosis and apoptosis. In conclusion, our results firstly demonstrated that the potential value of DHCR24-mediated regulation of cellular cholesterol level as a promising treatment for AD.

**Keywords** Alzheimer's disease, 24-dehydrocholesterol reductase (DHCR24), Cholesterol, Gene therapy, Neuroprotection, Neurodegeneration, Pathogenesis

## Introduction

So far, the amyloid hypothesis has dominated the research on Alzheimer's disease (AD) [27, 75]. However, the repeated failures of clinical trials targeting anti-amyloid-beta ( $A\beta$ ) have challenged our narrow understanding of AD pathogenesis, suggesting  $A\beta$  could be a prominent pathological feature but not exclusive causative factor, and inspiring wide-ranging investigations into the underlying mechanisms of AD [9, 32, 55, 64, 73, 77]. Although a number of hypotheses about the cause of AD have been proposed, the ultimate etiology of AD remains elusive [5, 6, 14, 27]. Because no effective treatments are still available for AD, the development of new disease-modifying treatment could become a really urgent need.

<sup>†</sup>Wen-bin Zhang and Yue Huang have contributed equally to this work.

\*Correspondence:

Xiang-shan Yuan  
yuanxiangshan1999@163.com

Heng-bing Zu  
hbzyy666@163.com

<sup>1</sup> Department of Neurology, Jinshan Hospital Affiliated to Fudan University, No.1508 Long-Hang Road, Jinshan District, Shanghai 201508, China

<sup>2</sup> Department of Anatomy and Histoembryology, School of Basic Medical Sciences, Fudan University, Shanghai 200032, China

<sup>3</sup> State Key Laboratory of Medical Neurobiology and Ministry of Education Frontiers Center for Brain Science, Institutes of Brain Science, Fudan University, Shanghai 200032, China



Interestingly, a tight link between AD neuropathology and lipid was proposed by Alois Alzheimer, who described “lipoid granules” as a third neuropathological hallmark of AD [26]. Since the early 1990s, many subjects have focused on the relationship between cholesterol metabolism and AD, including biology, epidemiology, and genetics [6, 10, 26, 47]. Although a few of researchers thought the high level of serum cholesterol was a hazard factor for AD, but it was ignored that the synthesis and supply or metabolism of cholesterol was independent in brain because of blood–brain barrier [6, 47, 61]. Thus, these evidences do not support the correlations between high plasma cholesterol and pathology of AD [6, 26, 47, 61]. Surprisingly, statins played beneficial role in many diseases by lowering serum cholesterol levels, but many studies also suggested it may show adverse effects due to the decrease of brain cholesterol levels [12, 45]. What’s more, Tamoxifen, which induced cognitive impairment in cancer therapy, was also found lead to cellular stress via inhibiting cholesterol synthesis [17].

Furthermore, accumulating data indicate a tight correlation between brain cholesterol deficiency and AD pathogenesis, which means forming a new cholesterol hypothesis [6, 10, 23, 47]. A growing body of evidences showed lower brain cholesterol, coupled with decreased cholesterol synthesis and trafficking in AD patients and animals, along with aging human and animals [6, 10, 35, 47, 52, 56, 57, 66, 83]. In addition, mutation or polymorphism of genes involving in brain cholesterol trafficking, including apolipoprotein E4 (APOE4), ATP binding cassette (ABC), low-density lipoprotein receptor (LDLR) family, and Niemann-Pick type C1/2 (NPC1/2), lead to reduced cholesterol efflux and transport and impaired cholesterol influx into neurons, eventually resulted in neuronal cholesterol deficiency, which could be tightly related to AD pathology, such as A $\beta$  deposition, phosphorylated tau accumulation, reactive astrogliosis, microglial phagocytosis, apoptosis and synaptic injuries [6, 10, 21, 42, 48, 71, 74].

What’s more, it was identified that 24-dehydrocholesterol reductase (DHCR24), a key regulator of synthesis and metabolism of cholesterol, was downregulated in vulnerable regions in AD patient brain [25, 31]. In previous *in vitro* studies, we demonstrated a loss in membrane and intracellular cholesterol by knocking down DHCR24, coupled with disruption of membrane lipid raft and abnormality of raft-dependent cell signaling, could leads to A $\beta$  generation, tau hyperphosphorylation, synaptic injuries and inflammation [6, 7, 49]. As a key enzyme in the biosynthesis of cholesterol, DHCR24 controlled cellular cholesterol synthesis and homeostasis [6]. Genetic evidences and outcomes from cell models strongly support cellular cholesterol deficiency contributes to AD

pathogenesis [6, 10]. Therefore, compelling evidences support a new hypothesis that brain cellular cholesterol loss could trigger the onset of AD.

To date, more and more therapy research focused on the cholesterol is coming to our attention. A possible treatment of AD of cholesterol-based gene therapy has been studied in many preclinical trials displaying inconsistent results [8, 29]. However, accumulating data suggests that ferrying the genes that are involved in cholesterol metabolism into mice brain could affect AD-related pathology and cognitive activity [8, 22, 29, 76]. Notably, in previous *in vitro* studies, we demonstrated that DHCR24 knock-in could alleviate AD-related pathological impairments by modulating the level of cellular cholesterol, including A $\beta$  generation, tau hyperphosphorylation, synaptic injuries, autophagy and apoptosis [6, 7, 15, 43, 49, 63]. As a key enzyme, DHCR24 could play a neuroprotective role in AD-related pathology by controlling cellular cholesterol synthesis and homeostasis [6]. In present study, we demonstrated the effect of DHCR24 in AD by AAV-mediated DHCR24 gene delivery in 5xFAD mice. Surprisingly, the cognitive impairment and AD-related pathology of 5xFAD mice was significantly reversed after DHCR24 knock-in. Taken together, based on the hypothesis of brain cellular cholesterol deficiency in AD, increasing evidences suggest that modifying brain cellular cholesterol metabolism by DHCR24 could provide a potential treatment for AD.

## Materials and methods

### Animals

5xFAD mice (male, 3 months, weight 17–23 g, Jackson Laboratory, 034848-JAX) and wild-type (WT) littermates were used in this experiment. The transgenic mice over-expressed both mutant human amyloid precursor protein (APP) and PS1 genes, which develop amyloid plaques and have a decline in long-term spatial working memory in 2 or 3 months, but not display neurofibrillary tangles [19]. With enough food or water, all mice were kept at the temperature of 22 °C in a 12–12 h light/dark cycle (lights on at 7 a.m. to 7 p.m., light intensity: 100 lx). Efforts were made into minimize animals used along with any pain experienced by mice as possible. All procedures and experiments were performed according to guidelines authorized by Animal Experiment and Use Committee at Shanghai Medical College of Fudan University (Permit No. 20210302-026).

### AAV injection and stereotaxic surgery

DHCR24 overexpression virus (AAV2/9-ZsGreen-DHCR24) and control virus (AAV2/9-ZsGreen), packaged and provided by Hanbio Tech (Shanghai, China), were injected into 5xFAD mice and WT mice (aged

3 months) under anesthesia of isoflurane via anesthesia mask. We used the following coordinates to inject AAV-DHCR24 cDNA or AAV-vector into bilateral hippocampus:  $-2.3$  mm anteroposterior and  $\pm 1.8$  mm mediolateral from the bregma, and  $-1.2$  mm dorsoventral from the surface of dura mater. Viral suspension ( $1 \mu\text{L}$ ) containing  $1.5 \times 10^{12}$  vector genomes per mL was placed into the target area at a rate of  $100 \text{ nL/min}$  by Using the Nanoject II (Drummond Scientific, Broomall, PA). After the injection, the pipette was retained for 15 min to allow absorption of AAV before being withdrawn. And then, keeping mice in a heater about 30–60 min to keep them warm during surgery. The mice underwent Morris water maze (MWM) 3–4 weeks after stereotactic injection, and were sacrificed at 7 days after the MWM testing.

#### Immunohistochemistry and immunofluorescence

One month after the AAV injection, the mice were anesthetized by using isoflurane via anesthesia mask. First, the transcardiac perfusion of mice was by  $0.01 \text{ M}$  phosphate-buffered saline (PBS) and then by  $4\%$  paraformaldehyde (PFA). Brains were carefully isolated and fixed in  $4\%$  PFA for 12–36 h at  $4 \text{ }^\circ\text{C}$ , finally placed them in  $30\%$  sucrose for 48–72 h at  $4 \text{ }^\circ\text{C}$ . All brains were prepared for frozen or paraffin sections according to experiments.

To the frozen sections, first brains should be embedded with OCT compound and be stored at  $-80 \text{ }^\circ\text{C}$ , and then were coronally sectioned at  $30 \mu\text{m}$  on a cryostat microtome (Leica 1950). The  $30 \mu\text{m}$  brain slices were collected in  $0.01 \text{ M}$  PBS and then be washed with PBS for three times. And then, the brain slices were incubated with  $3\%$  donkey serum (v/v),  $0.25\%$  Triton (v/v) and primary antibodies at  $4 \text{ }^\circ\text{C}$  overnight. Brain slices were then washed in PBS and incubated with Alexa 594 or Alexa 647 conjugated secondary antibodies (1:1000, Jackson ImmunoResearch) for 2 h in a room temperature (RT). Finally, brain slices were then washed again in PBS and cover-slipped with DAPI Fluoromount-G mounting medium (Southern Biotech, 0100-20). The fluorescence signals were detected by confocal microscope (Leica SP8, Germany) and VS120 virtual microscopy slide scanning system (Olympus), and the same parameters settings were employed between different groups.

To the paraffin sections, brains were embedded in paraffin wax, and cut into 4 microns-thick sections. After dewaxing, the brain slices were also incubated with  $3\%$  donkey serum (v/v),  $0.25\%$  Triton (v/v) and primary antibodies at  $4 \text{ }^\circ\text{C}$  overnight. Then incubated with biotinylated IgG (1:1000, Jackson ImmunoResearch) for 2 h in RT, and then incubated with ABC complex for 2 h in RT. Next, sections incubated with DAB ( $0.2 \text{ mg/ml}$ ) for 10 min in RT, and then mounted onto slides, dehydrated, and coverslipped.

Primary antibodies were used as follows: DHCR24 (1:500; ab137845, abcam); Beta Amyloid [MOAB-2] (1:400; ab126649, abcam); Synapsin I (1:500; ab64581, abcam); GFAP (1:2000; ab4674, abcam); NeuN (1:1000; ab177487, abcam); Iba1 (1:1000; PRB029, OasisBiofarm); CD68 (1:200; ab955, abcam).

#### Filipin III staining

Cholesterol level of hippocampus was evaluated by Filipin III staining. Brains embedded with OCT were coronally sectioned at  $10 \mu\text{m}$  on a cryostat microtome, then mounted onto slides, and then fixed by  $4\%$  PFA for 10 min. Sections were incubated in  $1.5\%$  glycine in PBS for 10 min followed by washed with PBS for three times. After 5 min washes in PBS for three times, sections were incubated for 2 h at RT with Filipin ( $0.05 \text{ mg/ml}$ ; SAE0087, Sigma) in PBS. After this, sections were washed with PBS again and coverslipped with fluorescent mounting media (DakoCytomation). The fluorescence signals of Filipin were detected by confocal microscope (Leica SP8, Germany) and the same settings were employed between different groups.

#### TUNEL staining

Apoptosis in the hippocampus was evaluated by TdT-mediated dUTP Nick-End Labeling (TUNEL) staining. Brains embedded with OCT were coronally sectioned at  $10 \mu\text{m}$  on a cryostat microtome, then mounted onto slides. Subsequently, the brain slices were incubated in  $0.5\%$  Triton for 10–20 min and then washed in PBS. We used One Step TUNEL Apoptosis Assay Kit (C1090, Beyotime Biotechnology, China),  $50 \mu\text{L}$  TUNEL reagent prepared as described in the instructions was added into each slice, and then slices were cultured in a dark environment at  $37 \text{ }^\circ\text{C}$  for 2 h. After washing PBS as above, slices were cover-slipped with DAPI Fluoromount-G mounting medium (Southern Biotech, 0100-20). The fluorescence signals were detected by confocal microscope (Leica SP8, Germany) and the same settings were employed between different groups.

#### Western blot

The animals were decapitated, separated hippocampus carefully, and then stored at  $-80 \text{ }^\circ\text{C}$ . Extracts from hippocampus were obtained in cold SDS lysis buffer (Merk, Shanghai), supplemented with both phosphatase inhibitor (1:100, Millipore) and protease inhibitor (1:100, Millipore). After centrifuged about 15 min at  $12,000 \times g$  (at  $4 \text{ }^\circ\text{C}$ ), the total protein concentration in tissue homogenates was detected by BCA assay kit (Thermo Scientific), and supernatants were then boiled for 5–10 min after mixing with loading buffer tricine (Takara). Subsequently, an equal amount

(20 ug) of proteins was fractionated by SDS PAGE on 10% or 12.5% polyacrylamide gels (PG112 and PG113, EpiZyme Biotechnology, China) according to their concentrations. Afterwards, proteins were transferred onto 0.2  $\mu\text{m}$  or 0.45  $\mu\text{m}$  PVDF membranes (Millipore) and then blocked with 5% skimmed milk in TBS containing 0.1% Tween 20 (TBST) at RT for 1 h. Besides, the bands were incubated with primary antibodies at 4 °C overnight. After washing the bands 3–4 times in TBST, then incubating it for 1 h at RT with secondary antibodies (1:5000, Proteintech, China) in Secondary Antibody Dilution Buffer (Beyotime, China). Finally, after washing again with TBST 3–4 times, the bands were detected by Immobilon ECL Ultra Western HRP (Millipore) and detected by Tannon 4600 Chemiluminescence Image Analysis System version 3.0 (Tannon, Shanghai, China). All experiments had been repeated at least 3 times.

Primary antibodies involved are as follows: DHCR24 (1:1000; ab137845, abcam); APP (1:1000; 2452S, Cell Signaling); SREBP2 (1:500; ab30682, abcam); HMGCR (1:800; DF6518, Affinity); Phospho-mTOR (1:1000; 5536S, Cell Signaling); mTOR (1:1000; 2983S, Cell Signaling); Phospho-GSK-3 $\beta$  (1:1000; 9323S, Cell Signaling); GSK-3 $\beta$  (1:1000; 12456S, Cell Signaling); Beclin-1 (1:1000; 3495S, Cell Signaling); SQSTM1/p62 (1:1000; 39749S, Cell Signaling); LC3B (1:1000; L7543, Sigma); Phospho-p38 MAPK (1:1000; 4511S, Cell Signaling); p38 MAPK (1:1000; 8690S, Cell Signaling); Phospho-JNK(1:1000; 4668S, Cell Signaling); JNK (1:1000; 9252S, Cell Signaling); Bax (1:1000; 5023S, Cell Signaling); Bim (1:1000; 2933S, Cell Signaling); Bcl2 (1:2000; 26593-1-AP, Proteintech); Caspase-3 (1:500; 19677-1-AP, Proteintech); Phospho-Erk1/2 (1:1000; 4370S, Cell Signaling); Erk1/2 (1:1000; 4695S, Cell Signaling); Phospho-MEK1/2 (1:1000; 9154S, Cell Signaling); MEK1/2 (1:1000; 8727S, Cell Signaling); RhoA (1:1000; 2117S, Cell Signaling); PSD95 (1:1000; 3409S, Cell Signaling); Synapsin I (1:2000; ab64581, abcam); HRP-conjugated GAPDH (1:10000; HRP-60004, Proteintech).

#### RT-PCR

Total RNA from hippocampus was isolated by the Total RNA extraction reagent RNAiso Plus (9108/9109, Takara, Japan). Reverse transcription used PrimeScript™ RT Master Mix (Takara, Japan) and PCR used TB Green Premix Ex (Takara, Japan). The threshold cycle (Ct) was acquired with Sequence Detection Software (Applied Biosystems, USA). The analysis of results was by  $\Delta\Delta\text{Ct}$  method and every target mRNA was normalized with the GAPDH. Primer sequences of DHCR24, HMGCR, SREBP2 and GAPDH were shown in Table 1.

**Table 1** List of primers and primer sequences

Genes	Forward primer (5'–3')	Reverse primer (5'–3')
DHCR24	CGCTGCGAGTCGGAAAGTA	GTCACCTGACCCATAGACACC
HMGCR	ATGCCTTGATTGGAGTTG	GTTACGGGGTTTGGTTTATT
SREBP2	GCAGCAACGGGACCATTCT	CCCCATGACTAAGTCTTCAACT
GAPDH	CTGCCAGAACATCATCC	CTCAGATGCCTGCTTAC

#### A $\beta$ ELISA

To detect the level of A $\beta$ 40 and A $\beta$ 42 in hippocampus, we separated the hippocampus and then stored at –80 °C. Extracts from hippocampus were obtained in cold SDS lysis buffer (Merk, Shanghai), supplemented with protease inhibitor (1:100, Millipore). After centrifuged for 15 min at 12000  $\times g$  (at 4 °C), the total protein concentration in tissue homogenates was determined using a BCA protein assay kit (Thermo Scientific). And then, the isolated protein samples were transferred to A $\beta$ 40 and A $\beta$ 42 ELISA kits (27,720 and 27,721, IBL, Japan), the measurement was according to protocol recommended by manufacturer. Most notably, the amount of A $\beta$ 40 and A $\beta$ 42 should be normalized with total protein concentration by BCA assay kits. These experiments duplicated at least 3 times and the data were acquired from independent experiments.

#### LC-MS/MS analysis

To detect the level of cholesterol in hippocampus, we separated the hippocampus for liquid chromatography-tandem mass spectrometry (LC-MS/MS) analysis. Cholesterol was extracted from measured amounts of material (at least 50 mg per sample), which means a sample included four hippocampi from 2 to 4 mice randomly from same group. Cholesterol extracts were prepared by chloroform–methanol extraction, added in proper internal standards, and analyzed by 1290/6490 Triple Quadrupole LC/MS system (Agilent Technologies). Cholesterol was separated with normal-phase HPLC using a Waters Cortecs column (2.7  $\mu\text{m}$  2.1  $\times$  100 mm Column) under the following conditions: mobile phase A (methanoic acid: water, 0.1:99.9, v/v) and mobile phase B (methanoic acid: methanol, 0.1:99.9, v/v); 95% A for 2 min, linear gradient to 30% A over 18 min and held for 3 min, and linear gradient to 95% A over 2 min and held for 6 min. Quantification of cholesterol was via multiple reaction monitoring. We measured the cholesterol in hippocampus by LC-MS/MS analysis, and the amount of cholesterol in every sample was normalized with their weight ( $\mu\text{g}/\text{mg}$  of wet tissue).



### Morris water maze

The MWM test to evaluate spatial learning consists of two consecutive stages: acquisition phase (AP) and space exploring test (SET) stage. Each mouse was given 4 trials per day for 5 days consecutive training with at least an hour intertrial interval. Each of the four starting positions was used randomly in daily trainings. In each trial, mice had 60 s to find platform in target quadrant. Trial was ended when mice arrived platform at least 3 s or time go to 60 s. When mice failed to find platform, they were guided to platform by experimenter and stayed about 20 s. Finally, space exploring test using trial as described previously but without the platform, and was 24 h later to the last training day. Tests were analyzed by Ethovision computerized tracking system (Noldus, Wageningen, Netherlands).

### Statistical analysis

All data were presented as mean  $\pm$  SEM. All data subjected to statistical analysis in GraphPad Prism 9 (GraphPad Software, La Jolla, CA). Statistical significance between 3 or 4 groups (except escape latency in MWM test) were detected by one-way ANOVA with Tukey's post hoc test. Statistical significance between two groups was analyzed by unpaired two-tailed Student's *t*-test. Three-way repeated measures ANOVA was used to analyze the results of escape latency in MWM test, and post-hoc comparison was performed by Fisher's least significant difference test. Differences with  $P < 0.05$  were considered to be significant, and significance expressed as follows: \* $P < 0.05$ , \*\* $P < 0.01$ , \*\*\* $P < 0.001$ .

## Results

### APP overexpression and/or A $\beta$ overload leads to significant decrease of hippocampal cholesterol level in 5xFAD mice

Noticeably, in FAD mice brain, the rapid increase of A $\beta$  could induce the inhibition of cholesterol synthetic genes, leading to cholesterol loss [6, 40, 71, 79]. And what's more, previous studies have showed that APP and A $\beta$ 40 or A $\beta$ 42 inhibited cholesterol synthesis and decreased cellular cholesterol level in neuron or glia [6, 40, 57, 79]. To better understand the hippocampal cholesterol metabolism state of the early symptomatic 5xFAD mice, we investigated whole-hippocampus cholesterol metabolism on 3-month-old WT and 5xFAD mice. Moreover, western blot and RT-PCR showed that the mRNA and protein level of main genes involving in cholesterol synthesis, including sterol regulatory element binding protein 2 (SREBP2), 3-hydroxy-3-methylglutaryl-CoA reductase (HMGCR), and DHCR24, was markedly down-regulated in hippocampus of 5xFAD mice compared to WT mice, indicating inhibition of

brain cholesterol synthesis (Fig. 1B–F). Furthermore, by a confocal laser scanning microscope, we observed that fluorescence intensity of the DHCR24 expression in hippocampus of 5xFAD mice was weaker than that of the age-matched WT mice, suggesting the decrease of hippocampal cholesterol synthesis (Fig. 1G). In contrast, immunofluorescence intensity analysis revealed that the level of hippocampal DHCR24 expression were lowered in the 5xFAD mice, indicating the decrease of hippocampal cholesterol biosynthesis level (Fig. 1H). Besides, compared with the WT mice, LC-MS/MS analysis indicated the cholesterol level of hippocampus is lower in 5xFAD mice (Fig. 1A).

Overall, based on previous research and our present study, we found the expression of essential genes involved in cholesterol synthesis were downregulated, resulting in a significant decrease of cholesterol level in the hippocampus of 5xFAD mice. Thus, a remarkable decrease in brain cholesterol level was appeared in the transgenic AD models, which means that these FAD mice are proper tools to investigate abnormal cholesterol metabolism associated with AD.

### DHCR24 overexpression increases cholesterol level in the hippocampus of 5xFAD mice and reverses cognitive impairment

To demonstrate the contribution of DHCR24 in improving the cognitive ability of AD, we employed delivery of AAV carrying DHCR24 gene into the hippocampus of 5xFAD mice at age of 3 months, and behavioral tests were performed at around 4-month-old (Fig. 2A). After DHCR24 transfection, the Filipin staining and LC-MS/MS analysis showed that the cholesterol level in the hippocampus of 5xFAD mice was up-regulated (Fig. 2B, C). To detect the effect of DHCR24 knock-in on cognition of 5xFAD mice, the Morris water maze (MWM) test was carried out [82]. The escape latency decreased significantly in 5xFAD-DHCR24 group after DHCR24 knock-in (Fig. 2D). The platform crossover number and the duration in target quadrant in 5xFAD-DHCR24 group were higher than that in the 5xFAD-control group (Fig. 2E, F). And the latency to platform and target quadrant decreased significantly after DHCR24 knock-in treatment in 5xFAD mice (Fig. 2G, K). The crossing number of target quadrant and duration in platform also significantly increased after DHCR24 overexpression in 5xFAD mice (Fig. 2I, J). In the trials, the swimming speed of mice in different groups was not significantly different (Fig. 2H). The results of MWM test suggested that DHCR24 knock-in effectively enhanced the cognitive ability of 5xFAD mice.

About one month after AAV injection, we detected ZsGreen fluorescence to verify successful injection, and

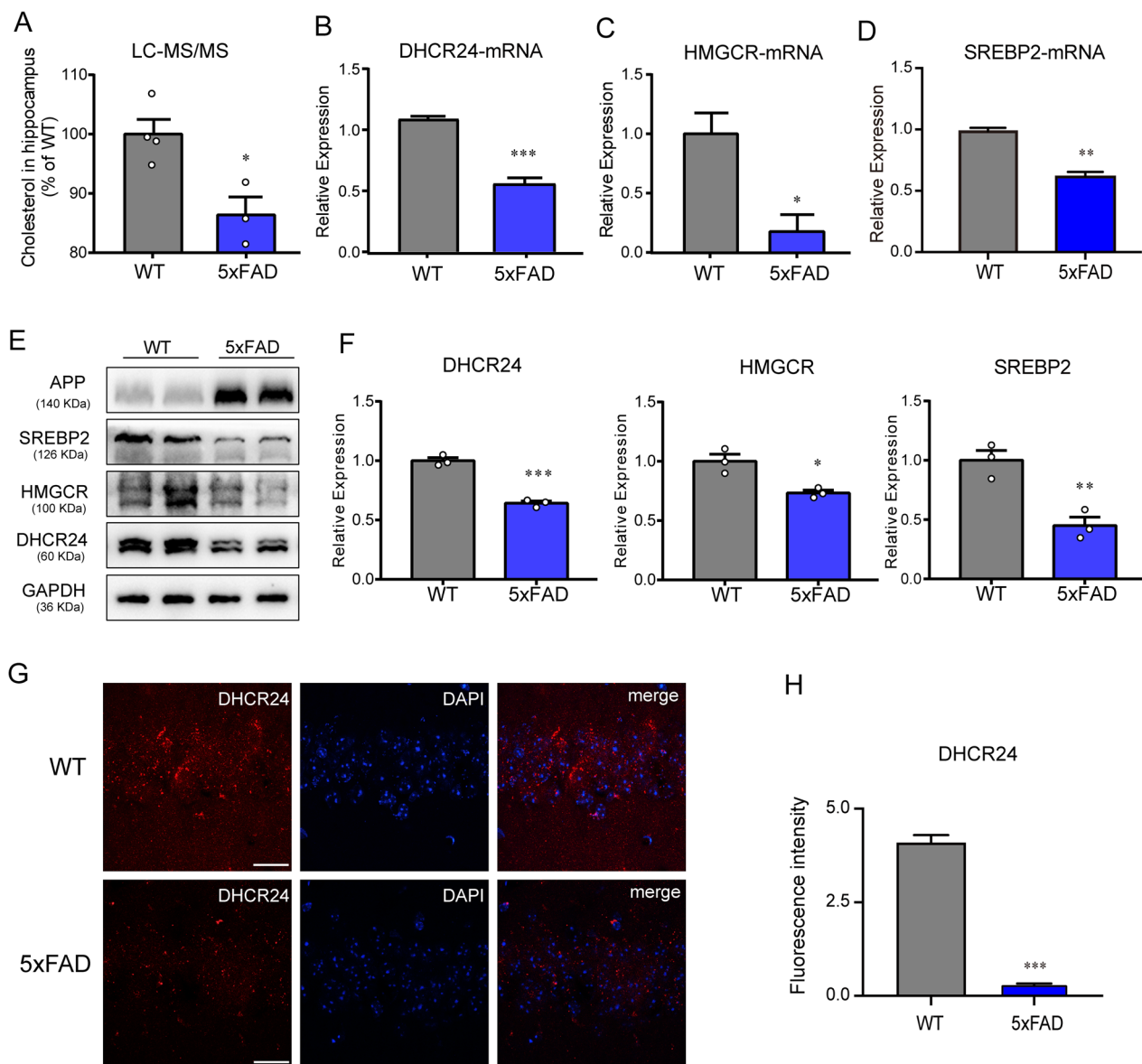


**Fig. 1** The significant decrease of hippocampal cholesterol level in 5xFAD mice. **A** Quantification of cholesterol level in hippocampus of WT and 5xFAD mice (3 month) by LC-MS/MS analysis.  $n=3-4$  sample/group, every sample was included 2-3 mice randomly. **B-D** The fold change expression of mRNA of DHCR24, HMGCR and SREBP2 in hippocampus of WT and 5xFAD mice (3 month) by RT-PCR. **E** The immunoblotting bands of DHCR24, HMGCR, SREBP2 in hippocampus of 3-month-old WT mice and 5xFAD mice. **F** Analysis of western blot with mean gray value which all were quantification on the ratio of target proteins against GAPDH. **G** The fluorescence images of DHCR24 (red) in hippocampus of 3-month-old WT and 5xFAD mice (scale bar, 20 μm). **H** Mean fluorescence intensity of DHCR24.  $n=3$  mice per group in [B-H]. Data expressed as mean  $\pm$  SEM, statistical analysis was performed using unpaired two-tailed Student's t-test. \* $P < 0.05$ ; \*\* $P < 0.01$ ; \*\*\* $P < 0.001$ ; compared with aged-matched WT group

found that ZsGreen is specifically expressed in the hippocampal CA1, CA2 and CA3 regions (Fig. 3C). After DHCR24 transfection, compared with 5xFAD-control mice, we found that DHCR24 is over-expressed in the neurons and astrocytes, as well as rarely in microglial cells, in the hippocampus of 5xFAD-DHCR24 group, indicating DHCR24 is successfully transfected (Fig. 3B,

F). Similarly, we found that DHCR24 is overexpressed in the hippocampal CA1, CA2, and CA3 regions of WT-DHCR24 group (Fig. 3A). RT-PCR and western blot analysis revealed the mRNA and protein level of DHCR24 expression in the hippocampus is increased by roughly 200 folds and by roughly 40 folds, respectively after DHCR24 knock-in treatment in 5xFAD mice (Fig. 3C-E).

Above data indicated DHCR24 overexpression in neurons and astrocytes could lead to the increase of astrocytic and neuronal cholesterol synthesis, resulting in elevated level of cellular cholesterol in the hippocampus. Overall, our outcomes suggested that DHCR24 knock-in could reverse the cognitive impairment of 5xFAD mice.

#### DHCR24 knock-in reduces A $\beta$ deposition in hippocampus of 5xFAD mice

Altered neuronal membrane cholesterol and/or sub-cellular level have been implicated in aberrant production and aggregation of A $\beta$  peptides [1, 6, 10, 15, 26, 47]. Interestingly, compared with 5xFAD-control group, we found DHCR24 overexpression decreased the A $\beta$  deposits and plaques in the hippocampal regions of 5xFAD mice (Fig. 4A–C). Further, the level of soluble A $\beta$ 42 and ratio of soluble A $\beta$ 42/A $\beta$ 40 is significantly lowered, and there's also a trend downward in the level of soluble A $\beta$ 40 in hippocampus of 5xFAD mice after DHCR24 knock-in (Fig. 4D–F). To sum up, our outcomes suggested that DHCR24 knock-in markedly reduced the content of soluble A $\beta$ 42 and A $\beta$  deposition. Of note, in neuronal and animal models, previous studies reported that deficiency of cellular cholesterol increased the generation of A $\beta$ 40 and A $\beta$ 42 [1, 6, 15]. Conversely, increasing cellular cholesterol level markedly reduced the production of A $\beta$ 40 and A $\beta$ 42 [1, 6, 15]. Very importantly, genetic evidences also support that neuronal cholesterol deficiency is associated with A $\beta$  production and accumulation, which is consistent with our present findings [6, 10, 21, 47, 71, 74]. Taking together, our findings revealed that increasing cellular cholesterol level by DHCR24 knock-in could prevent or reverse A $\beta$  deposition in 5xFAD mice.

#### DHCR24 knock-in reverses the inhibition of autophagy in 5xFAD mice

Autophagy is an important pathway for the clearance of aggregation-prone proteins including A $\beta$  involved in AD [39, 44, 59, 78]. In the initial step of autophagy, it involves numerous proteins such as the autophagy-related (ATG) proteins, which including Beclin-1 and microtubule associated protein 1 light chain 3 Alpha (LC3). Interestingly,

Beclin-1, which controlling an early step in the forms of autophagosome, was found to be downregulated in the brains of AD patients [39]. In our experiment, compared with the 5xFAD-control group, the expression of Beclin-1 and the LC3BII/LC3BI ratio increased in hippocampus of 5xFAD-DHCR24 group, implicating autophagy is activated (Fig. 4G–H). Furthermore, we found DHCR24 knock-in lowered the expression of Sequestosome1 (p62/SQSTM1), suggesting that degraded targets are recruited to autophagosomes via p62, a marker of autophagic activity (Fig. 4G, H).

In addition, the kinase mammalian target of rapamycin (mTOR) is an important regulator of the autophagy [6, 44]. And mTOR activity is modulated by upstream pathways, such as glycogen synthase kinase-3beta (GSK-3 $\beta$ ), which are regulated by DHCR24 [6, 78]. Here, we showed that 5xFAD mice had lower expression level of phosphorylated mTOR (p-mTOR) and higher expression level of phosphorylated GSK3 $\beta$  at Ser9 site after DHCR24 knock-in, suggesting DHCR24 overexpression induced the inhibition of mTOR signaling by GSK3 $\beta$  inactivation (Fig. 4G, H). Similarly, we also found DHCR24 overexpression activated autophagy by the cholesterol-mediated lipid-dependent mTOR signaling in cultured cells [6]. Moreover, it found that mTOR signaling regulates autophagy, and be inhibited in cortex or hippocampus of AD model mice [44, 78]. And autophagy disorder is a well consensus of participating mechanism in AD neuropathology, which is associated with memory impairment [44, 59, 78]. Therefore, our outcomes demonstrated DHCR24 knock-in could prevent or reverse the inhibition of AD-related autophagy in 5xFAD mice, at least partly via modulating cholesterol-mediated GSK3 $\beta$ /mTOR pathway.

#### DHCR24 overexpression reverses hippocampal synaptic injuries

Of note, previous studies confirmed that the formation of numerous and efficient synapses of neurons need gliasupplied cholesterol, which influencing basic synapse function, plasticity and behavior [50, 81]. Conversely, cellular cholesterol deficiency by genetic defects in cholesterol trafficking can impair synaptic growth and plasticity,

(See figure on next page.)

**Fig. 2** DHCR24 knock-in markedly improves cognitive ability of 5xFAD mice. **A** The timeline of the experiment and fluorescence images of ZsGreen (green) one month after AAV injection (scale bar, 200  $\mu$ m). **B** Fluorescence images of Filipin staining (blue) in the CA1 region of hippocampus (scale bar, 10  $\mu$ m) and the analysis results of mean fluorescence intensity which were normalized with 5xFAD-Control group. **C** Quantification of cholesterol level in hippocampus two groups by LC-MS/MS analysis which were normalized with 5xFAD-Control group. n = 3 sample/group, every sample was included 2–4 mice randomly. **D** Escape latency during the 5 days acquisition phase of Morris water maze (MWM) test. **E** The percentage of time spent in target quadrant in MWM test. **F** The number of platform crossings in MWM test. **G** The latency to platform in MWM test. **H** The swim speed of mice in MWM test. **I** The number of target quadrant crossings in MWM test. **J** The time spent in platform in MWM test. **K** The latency to the target quadrant in MWM test. n = 7–10 mice per group in [G], n = 8–10 mice per group in [D–F and H–K]. Data expressed as mean  $\pm$  SEM, statistical analysis between the five groups was analyzed by one-way ANOVA with Tukey's post hoc test, except for escape latency was analyzed by three-way repeated measures ANOVA with LSD post hoc test. \* $P < 0.05$ ; \*\* $P < 0.01$ ; \*\*\* $P < 0.001$ ; compared with aged-matched 5xFAD-Control group. The images of MWM trials were showed in Additional file 1: Fig. S1

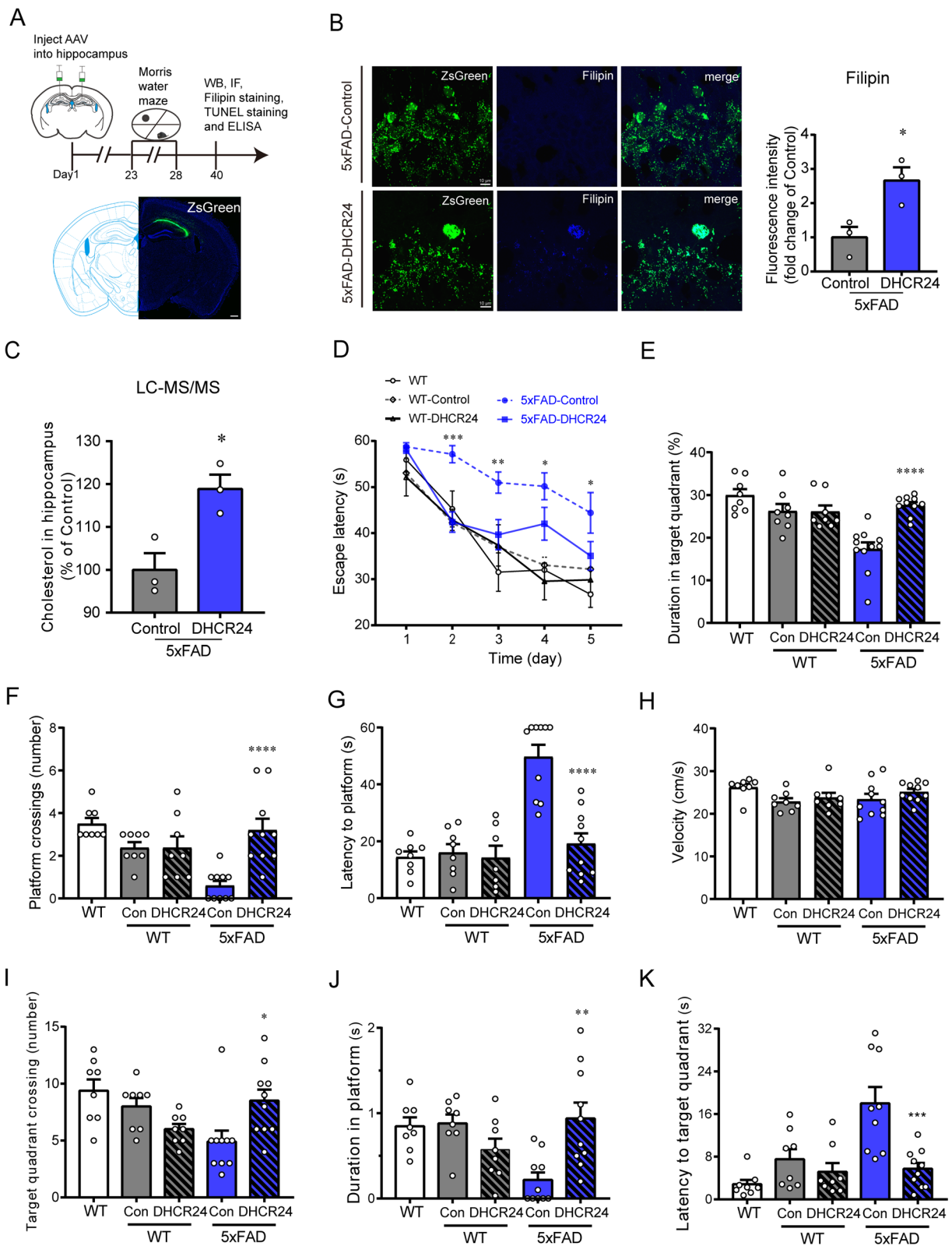


**Fig. 2** (See legend on previous page.)



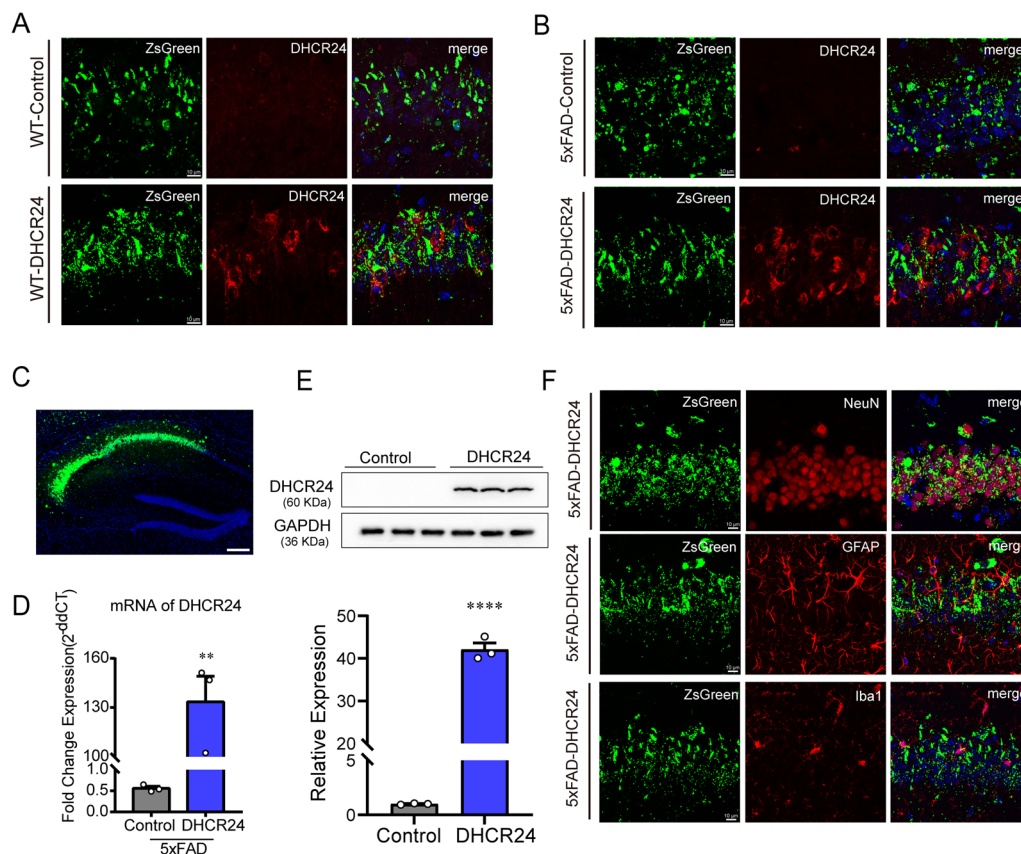


**Fig. 3** The over-expression of DHCR24 in the hippocampus of 5xFAD mice. **A, B** The fluorescence images of ZsGreen (green) and DHCR24 (red) in hippocampus (scale bar, 10  $\mu$ m). **C** Fluorescence image of ZsGreen (green) in hippocampus (scale bar, 200  $\mu$ m). **D** The fold change expression of mRNA of DHCR24 in hippocampus by RT-PCR. **E** The immunoblotting bands of DHCR24 protein and the analysis results of western blot with mean gray value which were quantification on the ratio of target proteins against GAPDH.  $n = 3$  mice per group. **F** Co-staining of ZsGreen (green) with NeuN (red) and GFAP (red) or Iba1 (red) in hippocampus (scale bar, 10  $\mu$ m). Data expressed as mean  $\pm$  SEM, statistical analysis between the two groups was analyzed by unpaired two-tailed Student's *t*-test. \* $P < 0.05$ ; \*\* $P < 0.01$ ; \*\*\* $P < 0.001$ ; compared with aged-matched 5xFAD-Control group

and synaptic function, such as transmission, and then contribute to cognitive deficits [10, 60, 81]. Here, the presynaptic marker synapsin-1 was performed in the hippocampal region by immunofluorescent (IF) staining (Fig. 5A–C). We observed that 5xFAD mice showed increased synapsin-1 immunoreactivity in the CA1, CA3, and dentate gyrus (DG) regions of hippocampus

after DHCR24 knock-in (Fig. 5A–C). And the IF analysis demonstrated that synapsin-1 in 5xFAD mice exhibited a 2.3-fold increase in the CA1 region, a 2.5-fold increase in the CA3 region and a 1.5-fold increase in the DG region after DHCR24 overexpression (Fig. 5D–F). However, there was no significant difference in synapsin-1 immunoreactivity in WT-control group and WT-DHCR24

(See figure on next page.)

**Fig. 4** DHCR24 knock-in alleviates A $\beta$  pathology and activates autophagy flux in hippocampus of 5xFAD mice. **A** The immunohistochemistry images of A $\beta$  plaques using the antibody MOAB-2 in the hippocampus (Scale bars, 200  $\mu$ m). Insets show a higher magnification of A $\beta$  plaques. Inset scale bar, 50  $\mu$ m. The right is analysis of number of A $\beta$  plaques in hippocampus.  $n = 12$  slices from 4 mice per group. **B** Fluorescence images of A $\beta$  (red) in prefrontal cortex and whole hippocampus (scale bar, 200  $\mu$ m). **C** The top half is the analysis of the area of A $\beta$  plaques, and the bottom half is the analysis of number of A $\beta$  plaques in prefrontal cortex and hippocampus.  $n = 7$  slices from 4 mice per group. **D, E** The relative level of A $\beta$ 42 and A $\beta$ 40 in hippocampus by ELISA which normalized with WT mice.  $n = 6$  mice per group. **F** The ratio of A $\beta$ 42/A $\beta$ 40 in hippocampus which normalized with WT mice. **G** The immunoblotting bands of p-mTOR, p-GSK3 $\beta$  (ser9), Beclin-1, P62 and LC3B in the hippocampus of 5xFAD-Control group and 5xFAD-DHCR24 group. **H** Analysis of western blot with mean gray value which all were quantification on the ratio of target proteins against GAPDH except p-mTOR and p-GSK3 $\beta$  (ser9) was against total mTOR and GSK3 $\beta$ ,  $n = 3$  mice per group. Data expressed as mean  $\pm$  SEM, statistical analysis between two groups was analyzed by unpaired two-tailed Student's *t*-test, between three groups was analyzed by one-way ANOVA with Tukey's post hoc test. \* $P < 0.05$ ; \*\* $P < 0.01$ ; \*\*\* $P < 0.001$ ; compared with aged-matched 5xFAD-Control group



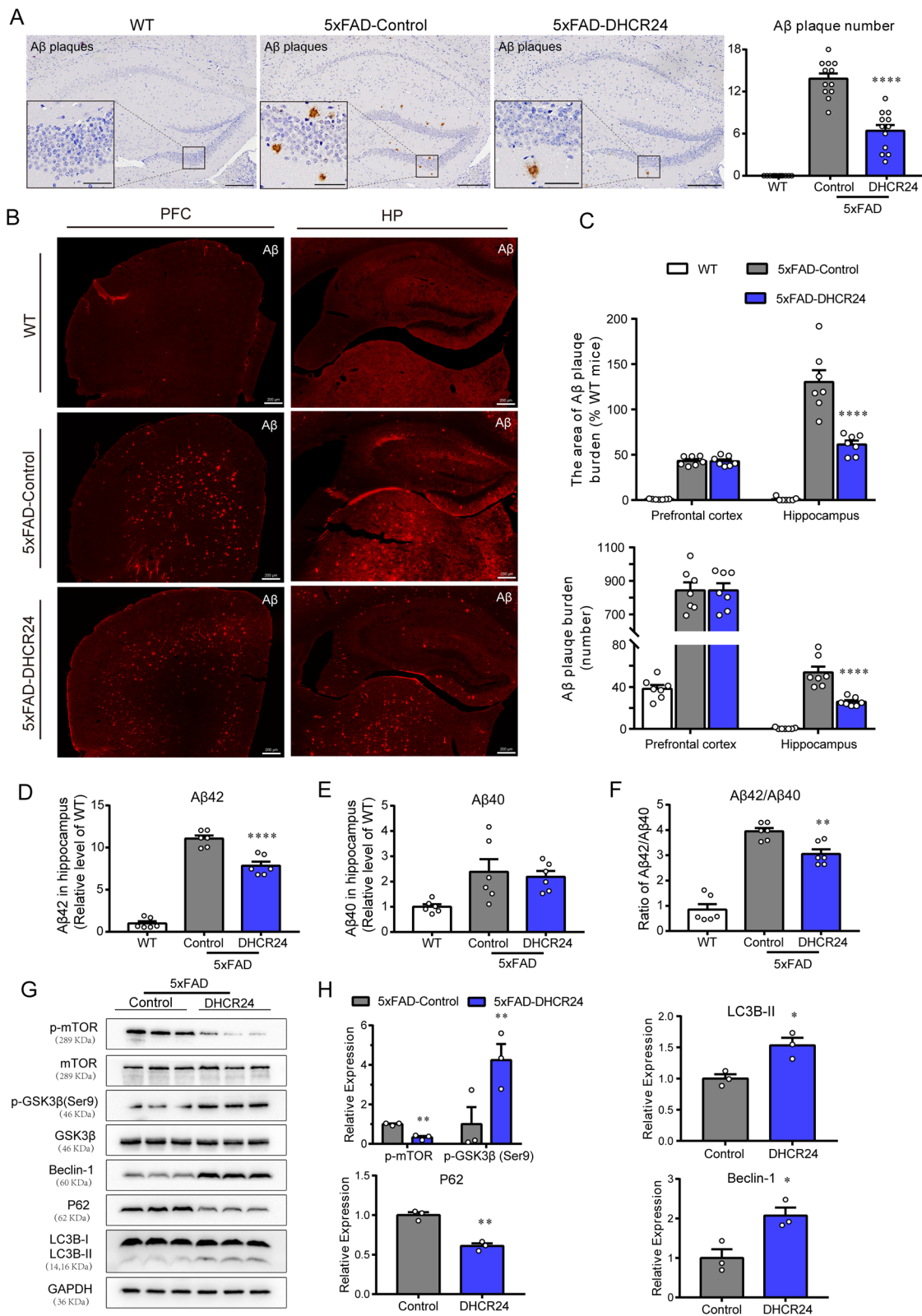


**Fig. 4** (See legend on previous page.)

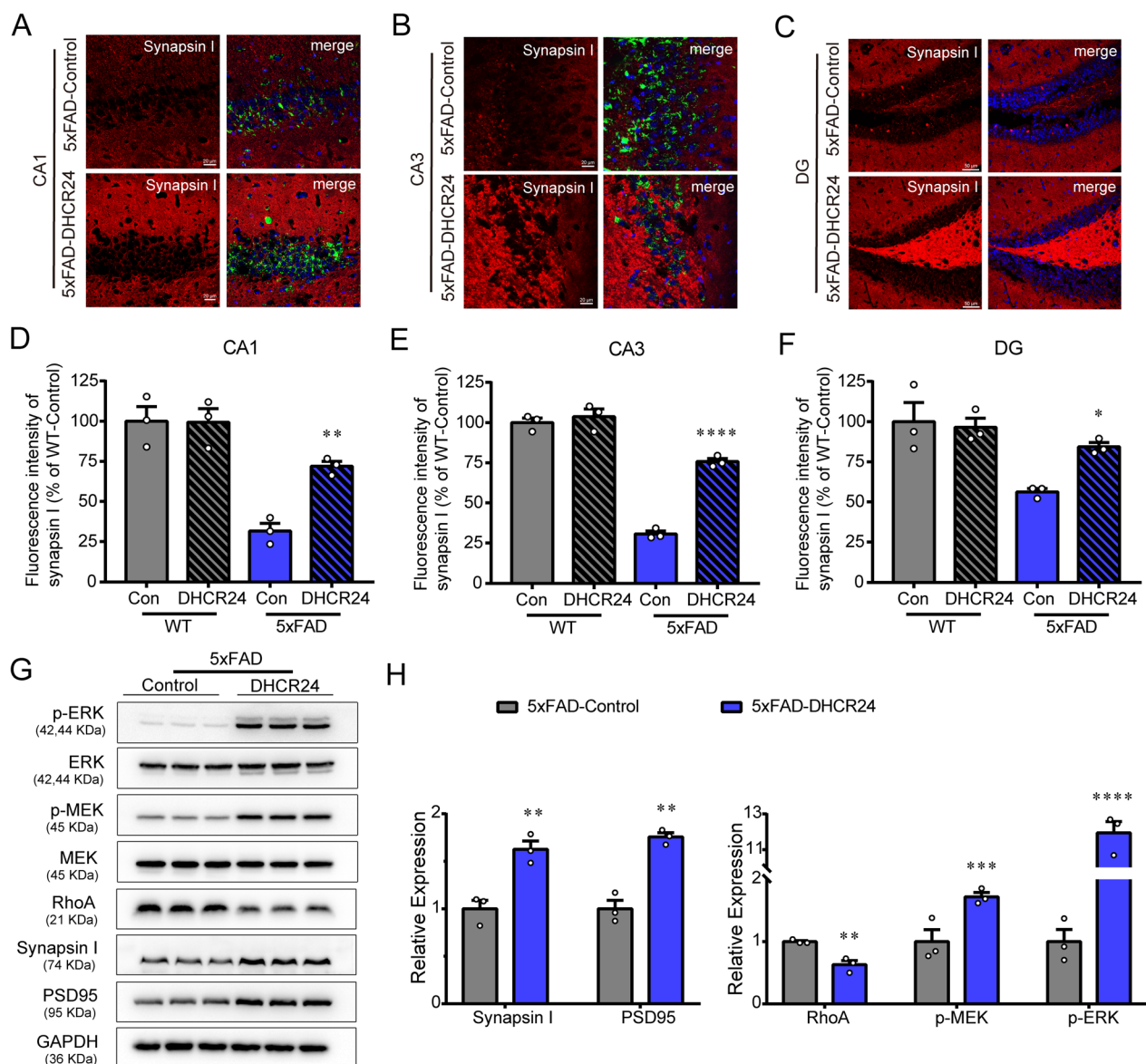


**Fig. 5** DHCR24 knock-in improves synaptic function in 5xFAD mice. **A, B** Fluorescence images of Synapsin I in the CA1 and CA3 region of hippocampus (scale bar, 20  $\mu$ m). **C** Fluorescence images of Synapsin I in the DG region of hippocampus (scale bar, 50  $\mu$ m). **D–F** Mean fluorescence intensity of Synapsin I in the CA1, CA3, and DG region.  $n=3$  mice/group. **G** The immunoblotting bands of PSD95, Synapsin I, RhoA, p-MEK and p-ERK in the hippocampus of 5xFAD-Control group and 5xFAD-DHCR24 group. **H** Analysis of western blot with mean gray value which all were quantification on the ratio of target proteins against GAPDH except p-MEK and p-ERK were the ratio against total MEK and ERK.  $n=3$  mice/group. Data expressed as mean  $\pm$  SEM, statistical analysis between the two groups was analyzed by unpaired two-tailed Student's t-test, between the four groups was analyzed by one-way ANOVA with Tukey's post hoc test. \* $P < 0.05$ ; \*\* $P < 0.01$ ; \*\*\* $P < 0.001$ ; compared with aged-matched 5xFAD-Control group. The images of Synapsin I in CA1, CA3 and DG regions of WT-Control group and WT-DHCR24 group were showed in Additional file 2: Fig. S2

group (Additional file 2: Fig. S2). Additionally, western blot analysis revealed that a dramatic increase in both the postsynaptic density 95 (PSD95) and synapsin-1 protein expression levels in hippocampus of 5xFAD mice after DHCR24 knock-in (Fig. 5G, H). Overall, our results revealed DHCR24 knock-in significantly reversed the decrease of PSD95 and synapsin-1 protein expression

in hippocampus of 5xFAD mice, suggesting the increase of synapse number in hippocampus. Notably, DHCR24 mutation or knockout leads to the loss of membrane cholesterol and disorder of lipid raft in the brain of patients and mice, resulting in synaptic abnormality and cognitive deficits [2, 6, 33, 65, 75, 88]. In contrast, DHCR24 knock-in increased the number of synapses in mouse

hippocampal neurons, promoting synapse formation [49]. Therefore, the increase of hippocampal neuronal cholesterol level by DHCR24 knock-in could promote synapse formation and maturation, and then improve the synapse function, which may be a mechanism by which cholesterol in plasma membrane affects synaptic transmission.

In addition, in the present study, DHCR24 knock-in increased the level of extracellular signal-related kinases 1 and 2 (ERK1/2) phosphorylation in the hippocampus of 5xFAD-DHCR24 group compared to 5xFAD-control group, suggesting ERK1/2 signaling was activated (Fig. 5G, H). ERK1/2 pathway regulated experience-dependent gene transcription, which has been proved to be essential to experience-related synaptic plasticity and formation of long-term memory [70]. Meanwhile, a significant decrease in RhoA levels in the Rho GTPase pathway was observed after DHCR24 knock-in treatment in 5xFAD mice (Fig. 5G, H). Collectively, our outcomes supported that DHCR24 knock-in regulated cholesterol-dependent lipid raft-related signals, including ERK1/2 and Rho-GTPase pathways in the hippocampus, which are involved in modulating synaptic plasticity and reconsolidation of memory in AD [3, 43, 70]. Hence, our outcomes supported that memory-enhancing activity could be associated with the enhancement of hippocampal synaptic function through DHCR24-mediated increase of cellular cholesterol level.

#### DHCR24 overexpression prevents hippocampal cellular apoptosis

Previous research revealed that DHCR24 can regulate cell survival and death, which is associated with the change of cellular cholesterol level [6, 67]. Here, we did not find any noticeable TUNEL-positive cells in the hippocampus of the WT-control or WT-DHCR24 group (Fig. 6A, B). In contrast, TUNEL-positive cells were more observed in the CA1 pyramidal cell layers in the 5xFAD-control group, suggesting abnormal apoptosis in hippocampus (Fig. 6A, B). Importantly, TUNEL positive cells were decreased in hippocampus of 5xFAD mice after DHCR24 knock-in treatment (Fig. 6A, B). Accordingly, these results revealed that DHCR24 knock-in prevented

or reversed apoptotic activity in the hippocampus of 5xFAD mice.

Intriguingly, the expression of B-cell lymphoma-2 (Bcl-2) family members, such as Bcl-2, Bcl-2-associated x protein (Bax), and building information modelling (Bim), was altered in AD brain, which controls cell death and survival processes by regulating mitochondrial outer membrane permeabilization [13, 68]. The mitogen-activated protein kinases (MAPK) family members, including c-Jun N-terminal kinase (JNK) and p38 kinase (P38), are known to regulate the activity of Bcl-2 family proteins [24, 68]. In our study, our results showed that the 5xFAD-DHCR24 group had lower levels of phosphorylated P38 (p-P38) and phosphorylated JNK (p-JNK), as well as higher level of Bcl-2 expression and lower levels of Bax and Bim expression (Fig. 6C). And the level of cleaved caspase-3 was markedly lowered in 5xFAD mice after DHCR24 knock-in (Fig. 6C). Furthermore, studies have shown that overexpression of DHCR24 protected cells from apoptosis by A $\beta$ -mediated toxicity, which is consistent with our present outcomes [6, 25, 37, 41, 67]. Thus, our data again confirmed that the anti-apoptotic effect of DHCR24 knock-in could be via P38 and JNK pathways which are regulated by cholesterol-dependent membrane lipid-rafts in the brain of 5xFAD mice.

#### DHCR24 overexpression inhibits reactive astrocytosis and promotes microglial phagocytosis

Previous research revealed that the A $\beta$  secreted from APP overexpressing transgenic mouse models could stimulate reactive astrocytosis, which contributes to progression of AD [34, 54, 58]. Here, the immunofluorescence staining of GFAP showed that DHCR24 knock-in inhibited reactive astrocytosis (Fig. 6D), which may be related to the reduction of A $\beta$  deposition. As for microglia, the phagocytic function was essential for the clearance of A $\beta$  plaques, and research found that phagocytic activity of microglia to the extracellular matrix could promote synapse plasticity in brain [16, 34, 54]. In present study, our results showed that the 5xFAD mice had higher rate of CD68 positive within Iba1 positive microglial cells after DHCR24 knock-in (Fig. 6E). As CD68 is a marker of active microglial phagocytosis [51, 69],

(See figure on next page.)

**Fig. 6** DHCR24 knock-in inhibits apoptosis or reactive astrocytosis and promotes microglial phagocytosis in 5xFAD mice. **A** Fluorescence images of TdT-mediated dUTP Nick-End Labeling (TUNEL) staining (red) in the CA1 region of hippocampus (scale bar, 20  $\mu$ m). **B** The ratio of TUNEL-positive cells against DAPI. **C** Representative immunoblotting bands of Cleaved caspase3, Bcl-2, Bim, Bax, p-JNK and p-P38 MAPK and analysis of western blot with mean gray value which all were quantification on the ratio of target proteins against GAPDH except p-JNK and p-P38 MAPK were against total JNK and P38 MAPK. **D** Co-staining of ZsGreen (green) with GFAP (red) in hippocampus and analyzing with the percentage of fluorescence area of GFAP (scale bar, 20  $\mu$ m). **E** Co-staining of Iba1 (green) with CD68 (red) in hippocampus and analyzing with the percentage of CD68+ positive within Iba1+ microglia (scale bar, 10  $\mu$ m). The arrows indicate CD68+ and Iba1+ microglia. n = 3 mice/group in [A-D], n = 6 brain slices from 3 mice/group in [E]. Data expressed as mean  $\pm$  SEM, statistical analysis between the two groups was analyzed by unpaired two-tailed Student's t-test, between the four groups was analyzed by one-way ANOVA with Tukey's post hoc test. \* $P$  < 0.05; \*\* $P$  < 0.01; \*\*\* $P$  < 0.001; compared with aged-matched 5xFAD-Control group

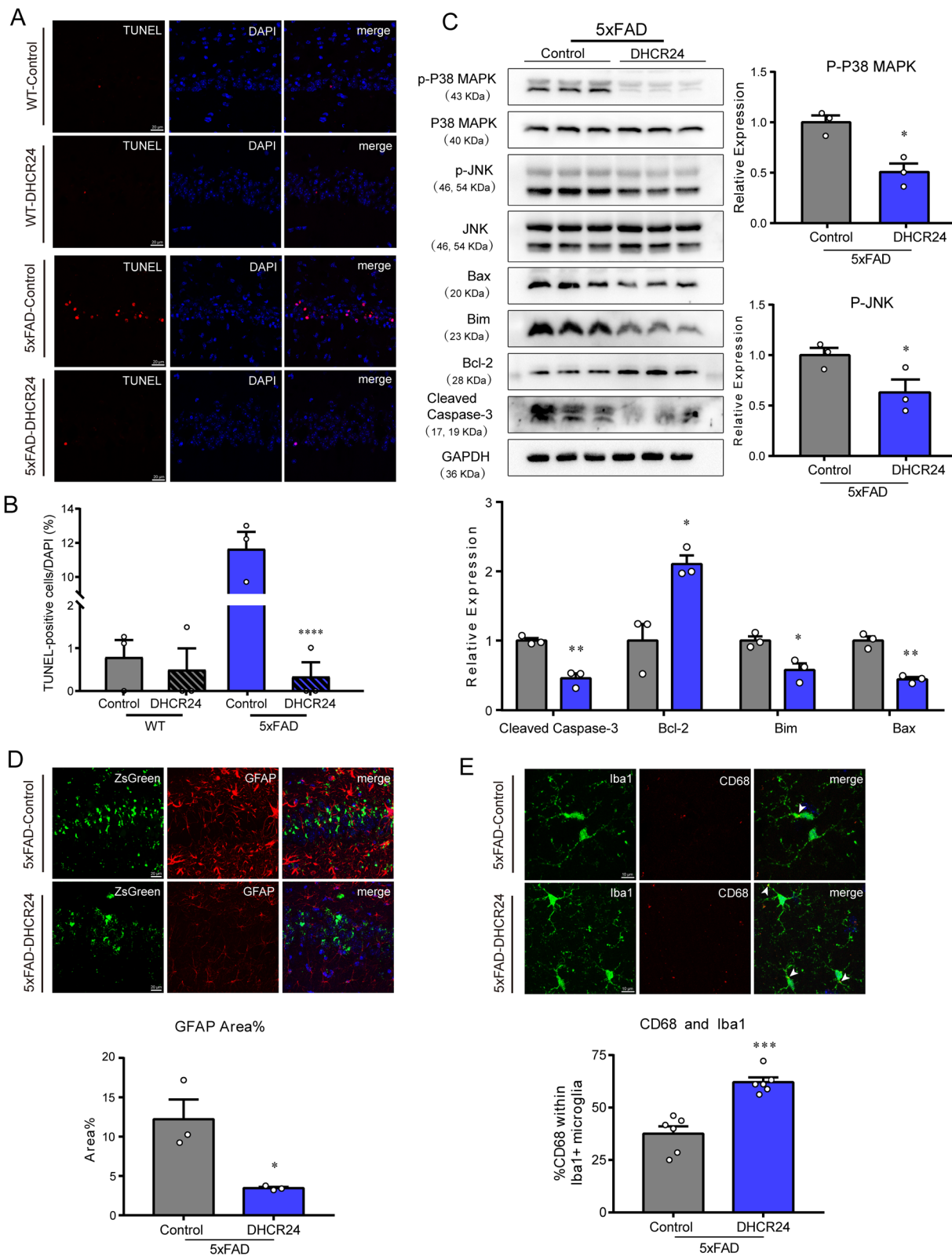


**Fig. 6** (See legend on previous page.)



above results suggested DHCR24 knock-in promoted microglial phagocytosis in 5xFAD mice (Fig. 6E). Thus, our data indicated that DHCR24 knock-in could inhibit reactive astrocytosis by increasing microglial-mediated clearance of A $\beta$ , and pro-phagocytic effects of DHCR24 could be the potential mechanism by which DHCR24 knock-in alleviates AD-related pathology and cognitive impairment.

## Discussion

In the present work, we found that there is a significant inhibition of hippocampal cholesterol biosynthesis, coupled with significantly decreased hippocampal cholesterol level in 5xFAD mice compared to age-matched WT mice (Fig. 1A–H). Moreover, the findings of our present study are consistent with previous research on FAD mice [6, 40, 57, 79]. In fact, APP overexpressing transgenic mouse models had lower level of cellular cholesterol in brain, and APP knockout mice had higher level of brain cellular cholesterol, which means that APP overexpression and/or A $\beta$  overload leads to brain cholesterol loss [40, 79]. Consequently, our findings suggested that the transgenic FAD mice, including 5xFAD mice, could be used as model to study brain cholesterol deficiency associated with AD. In order to test the AD-cholesterol hypothesis that brain cellular cholesterol deficiency triggers the onset and progression of AD, we conducted a new cholesterol-based DHCR24 gene therapy in 5xFAD mice (Fig. 2A). Surprisingly, by employing delivery of AAV9 carrying DHCR24 gene into the hippocampus of 5xFAD mice, we found that DHCR24 knock-in significantly reversed the cognitive impairment (Fig. 2D–K). Thus, our outcome firstly demonstrated that the potential value of DHCR24 knock-in as a promising treatment for AD.

Interestingly, we observed that DHCR24 is universally overexpressed in the hippocampal neurons and astrocytes of 5xFAD mice, coupled with the increase of cholesterol level in the hippocampus, indicating the increase of neuronal and astrocytic cholesterol synthesis in the hippocampus (Fig. 3B, F). In adult brain, the cholesterol-related activities of neurons are mainly supported by astrocyte-derived cholesterol, with a little part supported by cholesterol synthesized themselves [10, 21, 28, 62]. Accordingly, enhancement of DHCR24 function in the hippocampal neurons and astrocytes could induce an increase of cholesterol synthesis and supplementation, which could rectify the deficiency of neuronal cholesterol in 5xFAD mice brain (Fig. 7). Collectively, DHCR24 knock-in in astrocytes and neurons could increase cholesterol biosynthesis and rectify the situation of neuronal

cholesterol deficiency, and then impact aspects of neuronal dysfunction in 5xFAD mice model (Fig. 7).

Very interestingly, in present study, we showed that DHCR24 knock-in could obviously prevent or reverse AD-related pathology, including amyloid- $\beta$  deposition, synaptic injuries, inhibition of autophagy, and apoptosis, leading to a significant improvement in cognitive ability of 5xFAD model (Figs. 2, 3, 4, 5, 6, 7). Similarly, in vitro cultured cell models, previous studies have demonstrated that DHCR24 obviously could reverse AD-related pathological impairments by the increase of neuronal cellular cholesterol content [6, 7, 15, 36, 43, 50, 63]. Furthermore, within the brain, the majority of cholesterol is exited in cytoplasm, organelles and myelin sheaths [18, 61]. Neuronal morphology and function, as well as synaptic transmission, may require large amounts of cholesterol to maintain, as cholesterol was a vital membrane component and a regulator for signaling molecules [18, 81]. What's more, increasing evidences strongly supported that the deficiency in brain cellular cholesterol could contribute to AD-related pathology [2–4, 6, 7, 15, 21, 25, 26, 36, 37, 41, 43, 47, 50, 60, 63, 65, 80, 81, 88]. Therefore, our outcomes strongly indicated that DHCR24-mediated gene therapy could be a promising approach against AD via increasing neuronal cholesterol level.

The cholesterol in brain is about 23% of all in body [18, 28]. Mechanistically, brain cellular cholesterol is a useful molecule, which serves as initial membrane component, as a ligand or cofactor for proteins and as precursor for neurosteroid [6, 18, 30, 46, 53, 72, 81, 84]. Firstly, as an essential lipid molecule, cholesterol plays a critical role in the homeostasis of membrane structure and function. Moreover, cholesterol loss could lead to the disorders of lipid rafts and affect membrane-mediated cell activities and signaling transduction, such as membrane-related activity, and signaling including PI3K/Akt, GSK3, mTOR, MAPK/ERK, P38 MAPK, JNK, which has been linked to AD pathogenesis [6, 46, 53, 84]. Secondly, as a ligand or cofactor for proteins, the direct impact on free (unesterified) cholesterol on the structure and function of membrane proteins or intracellular proteins is recognized [20, 30, 72]. Moreover, it is found more than 250 candidate cholesterol-binding proteins in mammalian cells, including receptors, channels, and enzymes [30]. And free cholesterol may bind to proteins as a covalent or an allosteric modulator of protein function, such as G-protein coupled receptors (GPCR) and trafficking proteins and alters localization, transport or sorting of proteins between different organelles or membrane domains [20, 30, 72]. Thus, free cholesterol itself could directly regulate the structure or function of proteins by the specific interactions with proteins in mammalian cells, which could contribute to AD pathogenesis [6, 20, 30, 72]. Thirdly,



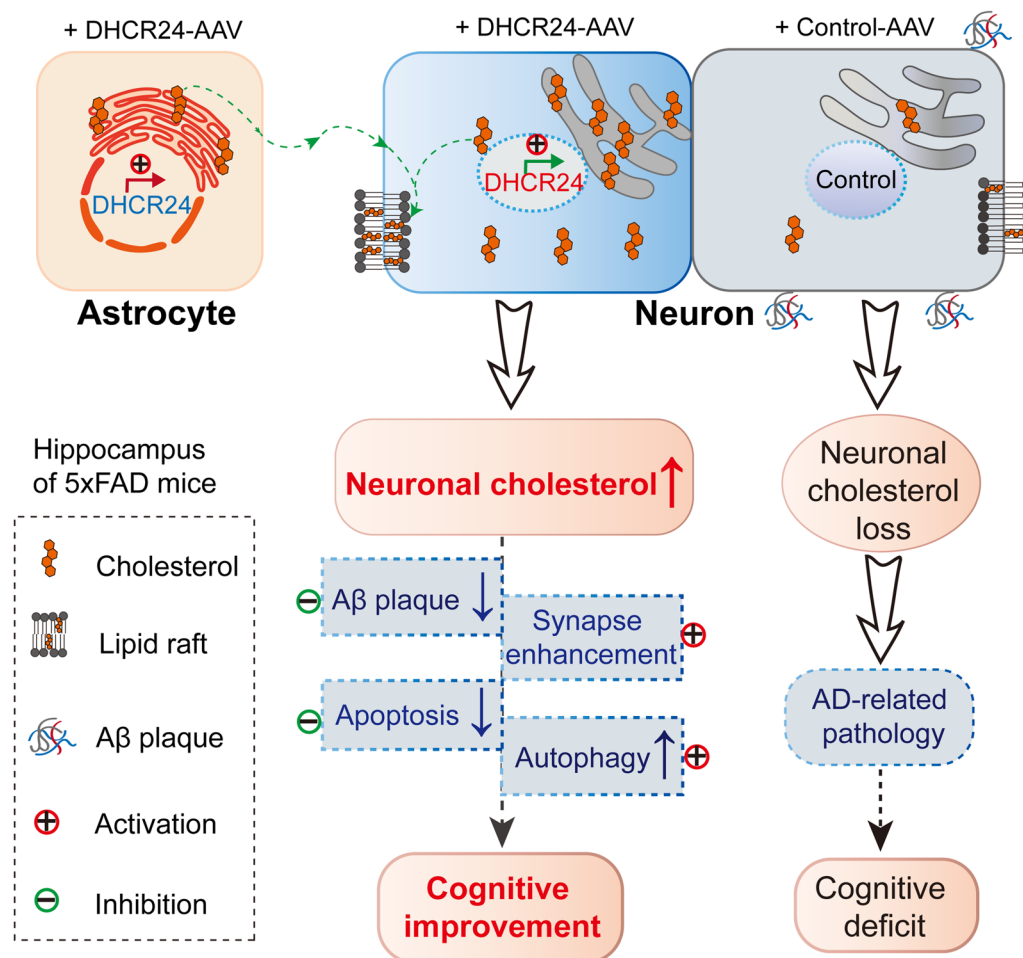


**Fig. 7** Schematic summary of DHCR24 knock-in reverses AD-related pathology and enhances cognitive ability of 5xFAD mice. To demonstrate the contribution of DHCR24 in improving the cognitive ability of AD, we employed delivery of adeno-associated virus (AAV) carrying DHCR24 gene into the hippocampus of 5xFAD mice. After DHCR24 transfection, DHCR24 is universally co-expressed in neurons and astrocytes, resulting in the increase of neuronal cholesterol level. By enhancing neuronal cholesterol level, DHCR24 knock-in successfully prevented or reversed AD-related pathology, including amyloid- $\beta$  deposition, synaptic injuries, inhibition of autophagy, and apoptosis. Finally, DHCR24 knock-in obviously improved the cognitive ability of 5xFAD mice

Cholesterol in the brain is also the precursor for neurosteroid biosynthesis [18, 28, 62, 81]. Previous data demonstrated neurosteroid hormone played a wide variety of essential protective and regulatory roles in the brain [11, 38, 85, 86]. The decrease or deficiency of neurosteroids in the brain is related to aging and neurodegenerative diseases, such as AD [38, 86]. Hence, increasing evidences strongly support that brain cholesterol plays a determined influence in brain development, homeostasis, and functional modulation.

Very importantly, our present study reflected on how DHCR24 knock-in markedly impacted critical aspects of AD pathology in 5xFAD model, which is consistent with previous studies in cell models, supporting brain cellular cholesterol is a key modulator of AD-related pathology

[6, 7, 10, 14, 15, 21, 36, 43, 47, 60, 63, 76, 80]. Intriguingly, on one hand, in many AD models and patients, increasing data indicated that the genetic and non-genetic risk factors for AD could lead to brain cholesterol deficiency, which means a direct causative link between brain cholesterol loss and AD (FAD and SAD) [6, 10, 21, 26, 47, 71, 74]. On the other hand, genetic evidences and outcomes from cell models strongly support cellular cholesterol deficiency contributes to AD pathological impairments [6, 10, 21, 71, 74]. Therefore, compelling evidences support that brain cellular cholesterol loss could induce the initiation and progression of AD [6]. Notably, in spite of etiology and background heterogeneous in FAD and SAD, the common pathological and clinical features for FAD and SAD support that the underlying mechanisms

of damage to neurons seem to be very similar [6, 10, 14, 36, 47, 60, 80]. Based on previous research and our present study, we concluded that neuronal cholesterol deficiency could play a critical role in modulating AD-related pathology, which is very likely to be a common node-point that triggers the initiation and progression of FAD and SAD. Therefore, our present study firstly demonstrated that brain cellular cholesterol deficiency could contribute to the pathogenesis of AD in 5xFAD model.

In summary, in present study, we showed cholesterol-based DHCR24 knock-in prevented or reversed AD-related pathology and effectively improved the cognitive impairment of 5xFAD mice by enhancement of neuronal cholesterol level. Consequently, encouraging results from our present study of DHCR24-targeted gene delivery in the brain could lead to the transition from pre-clinical to clinical trials. Besides, targeting the common node-point of brain cellular cholesterol deficiency, gene therapy might be a suitable treatment of AD compared to conventional therapy since it can be tailored to specifically alter AD-related pathological impairments, reverse disease phenotype and restore brain normal function. Thus, modulation of brain cellular cholesterol level by the target genes involving in cellular cholesterol synthesis or trafficking, such as HMGCR, DHCR24, APOE2, and LDLR, could be very valuable for preventing or reversing AD pathology [3, 6, 29, 33, 76, 87]. Accordingly, the rectification of cellular cholesterol deficiency/loss in AD brain could be a potential treatment to prevent or slow the neurodegeneration of AD.

#### Abbreviations

AAV	Adeno-associated virus
ABC	ATP binding cassette
A $\beta$	Amyloid- $\beta$
AD	Alzheimer's disease
APOE4	Apolipoprotein E4
APP	Amyloid precursor protein
ATG	Autophagy-related protein
Bax	BCL-2-Associated X Protein
Bcl-2	B-cell lymphoma-2
Bim	Bcl-2 interacting mediator of cell death
DHCR24	24-Dehydrocholesterol reductase
ERK1/2	Extracellular-regulated kinase 1/2
FAD	Familial Alzheimer's disease
GPCR	G-protein coupled receptors
GSK-3 $\beta$	Glycogen synthase kinase-3beta
HMGCR	3-Hydroxy-3-methylglutaryl-CoA reductase
LC3	Microtubule associated protein 1 light chain 3 Alpha
LC-MS/MS	Liquid chromatography-tandem mass spectrometry
LDLR	Low-density lipoprotein receptor
IF	Immunofluorescent
JNK	C-Jun N-terminal kinase
MAPK	Mitogen-activated protein kinases
mTOR	Mammalian target of rapamycin
MWM	Morris water maze
NPC1/2	Niemann Pick type C1/2
p62/SQSTM1	Sequestosome1

p38 MAPK	P38 mitogen activated protein kinases
PSD95	Postsynaptic density 95
SREBP2	Sterol regulatory element binding protein 2
SAD	Sporadic Alzheimer's disease
Tau	Microtubule-associated protein tau
TUNEL	DTdT-mediated dUTP Nick-End Labeling
WT	Wild-type

## Supplementary Information

The online version contains supplementary material available at <https://doi.org/10.1186/s40478-023-01593-y>.

**Additional file 1: Fig. S1.** Representative images of the Morris water maze trials of the mice of five groups

**Additional file 2: Fig. S2.** The effect of DHCR24 knock-in on Synapsin I in the hippocampus of WT mice. **A** Fluorescence images of Synapsin I in the CA1 region in WT-Control group and WT-DHCR24 group. **B** Mean fluorescence intensity of Synapsin I in the CA1 region. **C** The images of Synapsin I in the CA3 region in WT-Control group and WT-DHCR24 group. **D** Mean fluorescence intensity of Synapsin I in the CA3 region. **E** Fluorescence images of Synapsin I in the DG region. **F** Mean fluorescence intensity of Synapsin I in the DG region. n = 3 mice per group in [A-F]. Data expressed as mean  $\pm$  SEM, statistical analysis between the two groups was analyzed by unpaired two-tailed Student's t-test. \* $P < 0.05$ ; \*\* $P < 0.01$ ; \*\*\* $P < 0.001$ ; compared with aged-matched WT-Control group

#### Acknowledgements

We thank the support from the innovative research team of high-level local university in Shanghai.

#### Author contributions

WZ and YH contributed equally to this work. HZ conceived and designed the study. XY partly designed the study and performed the experiments. WZ and YH performed the majority of experiments. MZ and XG partly performed the experiments. HZ, XY, WZ, and YH analyzed the data. HZ and WZ wrote the manuscript. All authors discussed the results and commented on the manuscript.

#### Funding

This work was supported by the Shanghai Health and Medical Development Foundation, Shanghai, China (201740209); the Jinshan Hospital affiliated to Fudan University Development Foundation, Shanghai, China (HBXK-2022-2); the National Natural Science Foundation of China (31971110, 32171142); the Shanghai Jinshan District Key Medical Foundation, Shanghai, China (JSZK2015A05 and JSZK2019A06); Open Project of Key Laboratory of Longevity and Aging-related Diseases (Guangxi Medical University), Ministry of Education (KLLAD202201).

#### Availability of data and materials

This study includes no data deposited in external repositories. Expanded View for this article is available online. DHCR24 gene source data, other data that support the findings of this study are available from the corresponding author upon reasonable request.

#### Declarations

##### Ethics approval and consent to participate

This research project was carried out according to guidelines authorized by Animal Experiment and Use Committee at Shanghai Medical College of Fudan University (Permit No. 20210302-026).

##### Consent for publication

Not applicable.

##### Competing interests

The authors have declared that no conflict of interest exists.

Received: 1 April 2023 Accepted: 30 May 2023  
Published online: 21 June 2023

## References

- Abad-Rodriguez J, Ledesma MD, Craessaerts K, Perga S, Medina M, Delacourte A, Dingwall C, De Strooper B, Dotti CG (2004) Neuronal membrane cholesterol loss enhances amyloid peptide generation. *J Cell Biol* 167:953–960. <https://doi.org/10.1083/jcb.200404149>
- Allen LB, Genaro-Mattos TC, Porter NA, Mirnics K, Korade Z (2019) Desmosterolosis and desmosterol homeostasis in the developing mouse brain. *J Inherit Metab Dis* 42:934–943. <https://doi.org/10.1002/jimd.12088>
- Anchisi L, Dessi S, Pani A, Mandas A (2012) Cholesterol homeostasis: a key to prevent or slow down neurodegeneration. *Front Physiol* 3:486. <https://doi.org/10.3389/fphys.2012.00486>
- Andersson HC, Kratz L, Kelley R (2002) Desmosterolosis presenting with multiple congenital anomalies and profound developmental delay. *Am J Med Genet* 113:315–319. <https://doi.org/10.1002/ajmg.b.10873>
- Attems J, Jellinger KA (2013) Amyloid and tau: neither chicken nor egg but two partners in crime! *Acta Neuropathol* 126:619–621. <https://doi.org/10.1007/s00401-013-1167-9>
- Bai X, Mai M, Yao K, Zhang M, Huang Y, Zhang W, Guo X, Xu Y, Zhang Y, Qurban A et al (2022) The role of DHCR24 in the pathogenesis of AD: re-cognition of the relationship between cholesterol and AD pathogenesis. *Acta Neuropathol Commun* 10:35. <https://doi.org/10.1186/s40478-022-01338-3>
- Bai X, Wu J, Zhang M, Xu Y, Duan L, Yao K, Zhang J, Bo J, Zhao Y, Xu G et al (2021) DHCR24 knock-down induced tau hyperphosphorylation at Thr181, Ser199, Thr231, Ser262, Ser396 epitopes and inhibition of autophagy by overactivation of GSK3beta/mTOR signaling. *Front Aging Neurosci* 13:513605. <https://doi.org/10.3389/fnagi.2021.513605>
- Barbero-Camps E, Fernandez A, Martinez L, Fernandez-Checa JC, Colell A (2013) APP/PS1 mice overexpressing SREBP-2 exhibit combined Abeta accumulation and tau pathology underlying Alzheimer's disease. *Hum Mol Genet* 22:3460–3476. <https://doi.org/10.1093/hmg/ddt201>
- Behl C, Ziegler C (2017) Beyond amyloid—widening the view on Alzheimer's disease. *J Neurochem* 143:394–395. <https://doi.org/10.1111/jnc.14137>
- Borras C, Mercer A, Sirisi S, Alcolea D, Escola-Gil JC, Blanco-Vaca F, Tondo M (2022) HDL-like-mediated cell cholesterol trafficking in the central nervous system and Alzheimer's disease pathogenesis. *Int J Mol Sci*. <https://doi.org/10.3390/ijms23169356>
- Bu J, Zu H (2014) Effects of pregnenolone intervention on the cholinergic system and synaptic protein 1 in aged rats. *Int J Neurosci* 124:117–124. <https://doi.org/10.3109/00207454.2013.824437>
- Butterfield DA, Barone E, Mancuso C (2011) Cholesterol-independent neuroprotective and neurotoxic activities of statins: perspectives for statin use in Alzheimer disease and other age-related neurodegenerative disorders. *Pharmacol Res* 64:180–186. <https://doi.org/10.1016/j.phrs.2011.04.007>
- Callens M, Kraskovskaya N, Derevtsova K, Annaert W, Bultynck G, Bezprozvanny I, Vervliet T (2021) The role of Bcl-2 proteins in modulating neuronal Ca<sup>2+</sup> signaling in health and in Alzheimer's disease. *Biochim Biophys Acta Mol Cell Res* 1868:118997. <https://doi.org/10.1016/j.bbamcr.2021.118997>
- Castello MA, Soriano S (2013) Rational heterodoxy: cholesterol reformation of the amyloid doctrine. *Ageing Res Rev* 12:282–288. <https://doi.org/10.1016/j.jarr.2012.06.007>
- Cramer A, Biondi E, Kuehnle K, Lutjohann D, Thelen KM, Perga S, Dotti CG, Nitsch RM, Ledesma MD, Mohajeri MH (2006) The role of seladin-1/DHCR24 in cholesterol biosynthesis, APP processing and Abeta generation in vivo. *EMBO J* 25:432–443. <https://doi.org/10.1038/sj.emboj.7600938>
- De Schepper S, Ge JZ, Crowley G, Ferreira LSS, Garceau D, Toomey CE, Sokolova D, Rueda-Carrasco J, Shin SH, Kim JS et al (2023) Perivascular cells induce microglial phagocytic states and synaptic engulfment via SPP1 in mouse models of Alzheimer's disease. *Nat Neurosci* 26:406–415. <https://doi.org/10.1038/s41593-023-01257-z>
- Denk F, Ramer LM, Erskine EL, Nassar MA, Bogdanov Y, Signore M, Wood JN, McMahon SB, Ramer MS (2015) Tamoxifen induces cellular stress in the nervous system by inhibiting cholesterol synthesis. *Acta Neuropathol Commun* 3:74. <https://doi.org/10.1186/s40478-015-0255-6>
- Dietschy JM, Turley SD (2004) Thematic review series: brain Lipids. Cholesterol metabolism in the central nervous system during early development and in the mature animal. *J Lipid Res* 45:1375–1397. <https://doi.org/10.1194/jlr.R400004-JLR200>
- Drummond E, Wisniewski T (2017) Alzheimer's disease: experimental models and reality. *Acta Neuropathol* 133:155–175. <https://doi.org/10.1007/s00401-016-1662-x>
- Fantini J, Epand RM, Barrantes FJ (2019) Cholesterol-recognition motifs in membrane proteins. *Adv Exp Med Biol* 1135:3–25. [https://doi.org/10.1007/978-3-030-14265-0\\_1](https://doi.org/10.1007/978-3-030-14265-0_1)
- Fernandez-Calle R, Konings SC, Frontinan-Rubio J, Garcia-Revilla J, Campubi-Ferrer L, Svensson M, Martinson I, Boza-Serrano A, Venero JL, Nielsen HM et al (2022) APOE in the bulls-eye of neurodegenerative diseases: impact of the APOE genotype in Alzheimer's disease pathology and brain diseases. *Mol Neurodegener* 17:62. <https://doi.org/10.1186/s13024-022-00566-4>
- Ferris HA, Perry RJ, Moreira GV, Shulman GI, Horton JD, Kahn CR (2017) Loss of astrocyte cholesterol synthesis disrupts neuronal function and alters whole-body metabolism. *Proc Natl Acad Sci U S A* 114:1189–1194. <https://doi.org/10.1073/pnas.1620506114>
- Gliozzi M, Musolino V, Bosco F, Scicchitano M, Scarano F, Nucera S, Zito MC, Ruga S, Carresi C, Macri R et al (2021) Cholesterol homeostasis: researching a dialogue between the brain and peripheral tissues. *Pharmacol Res* 163:105215. <https://doi.org/10.1016/j.phrs.2020.105215>
- Goel P, Chakrabarti S, Goel K, Bhutani K, Chopra T, Bali S (2022) Neuronal cell death mechanisms in Alzheimer's disease: an insight. *Front Mol Neurosci* 15:937133. <https://doi.org/10.3389/fnmol.2022.937133>
- Greeve I, Hermans-Borgmeyer I, Brellinger C, Kasper D, Gomez-Isla T, Behl C, Levkau B, Nitsch RM (2000) The human DIMINUTO/DWARF1 homolog seladin-1 confers resistance to Alzheimer's disease-associated neurodegeneration and oxidative stress. *J Neurosci* 20:7345–7352. <https://doi.org/10.1523/JNEUROSCI.20-19-07345.2000>
- Grimm MO, Mett J, Grimm HS, Hartmann T (2017) APP function and lipids: a bidirectional link. *Front Mol Neurosci* 10:63. <https://doi.org/10.3389/fnmol.2017.00063>
- Hardy JA, Higgins GA (1992) Alzheimer's disease: the amyloid cascade hypothesis. *Science* 256:184–185. <https://doi.org/10.1126/science.1566067>
- Hayashi H (2011) Lipid metabolism and glial lipoproteins in the central nervous system. *Biol Pharm Bull* 34:453–461. <https://doi.org/10.1248/bpb.34.453>
- Hu J, Liu CC, Chen XF, Zhang YW, Xu H, Bu G (2015) Opposing effects of viral mediated brain expression of apolipoprotein E2 (apoE2) and apoE4 on apoE lipidation and Abeta metabolism in apoE4-targeted replacement mice. *Mol Neurodegener* 10:6. <https://doi.org/10.1186/s13024-015-0001-3>
- Hulce JJ, Cognetta AB, Niphakis MJ, Tully SE, Cravatt BF (2013) Proteome-wide mapping of cholesterol-interacting proteins in mammalian cells. *Nat Methods* 10:259–264. <https://doi.org/10.1038/nmeth.2368>
- Iivonen S, Hiltunen M, Alafuzoff I, Mannermaa A, Kerokoski P, Puolivali J, Salminen A, Helisalmi S, Soininen H (2002) Seladin-1 transcription is linked to neuronal degeneration in Alzheimer's disease. *Neuroscience* 113:301–310. [https://doi.org/10.1016/s0306-4522\(02\)00180-x](https://doi.org/10.1016/s0306-4522(02)00180-x)
- Karran E, De Strooper B (2016) The amyloid cascade hypothesis: are we poised for success or failure? *J Neurochem* 139(Suppl 2):237–252. <https://doi.org/10.1111/jnc.13632>
- Kim J, Castellano JM, Jiang H, Basak JM, Parsadanian M, Pham V, Mason SM, Paul SM, Holtzman DM (2009) Overexpression of low-density lipoprotein receptor in the brain markedly inhibits amyloid deposition and increases extracellular A beta clearance. *Neuron* 64:632–644. <https://doi.org/10.1016/j.neuron.2009.11.013>
- Kleffman K, Levinson G, Rose IVL, Blumenberg LM, Shadaloey SAA, Dhabaria A, Wong E, Galan-Echevarria F, Karz A, Argibay D et al (2022) Melanoma-secreted amyloid beta suppresses neuroinflammation and

- promotes brain metastasis. *Cancer Discov* 12:1314–1335. <https://doi.org/10.1158/2159-8290.CD-21-1006>
35. Kolsch H, Heun R, Jessen F, Popp J, Hentschel F, Maier W, Lutjohann D (2010) Alterations of cholesterol precursor levels in Alzheimer's disease. *Biochim Biophys Acta* 1801:945–950. <https://doi.org/10.1016/j.bbali.2010.03.001>
  36. Koudinov AR, Koudinova NV (2005) Cholesterol homeostasis failure as a unifying cause of synaptic degeneration. *J Neurol Sci* 229–230:233–240. <https://doi.org/10.1016/j.jns.2004.11.036>
  37. Kuehnl K, Cramer A, Kalin RE, Luciani P, Benvenuti S, Peri A, Ratti F, Rodolfo M, Kulic L, Heppner FL et al (2008) Prosurvival effect of DHCR24/Seladin-1 in acute and chronic responses to oxidative stress. *Mol Cell Biol* 28:539–550. <https://doi.org/10.1128/MCB.00584-07>
  38. Lloyd-Evans E, Waller-Evans H (2020) Biosynthesis and signalling functions of central and peripheral nervous system neurosteroids in health and disease. *Essays Biochem* 64:591–606. <https://doi.org/10.1042/EBC20200043>
  39. Loera-Valencia R, Piras A, Ismail MAM, Manchanda S, Eijolfssdottir H, Saido TC, Johansson J, Eriksdottir M, Winblad B, Nilsson P (2018) Targeting Alzheimer's disease with gene and cell therapies. *J Intern Med* 284:2–36. <https://doi.org/10.1111/joim.12759>
  40. Loffler T, Schweinzer C, Flunkert S, Santha M, Windisch M, Steyrer E, Hutter-Paier B (2016) Brain cortical cholesterol metabolism is highly affected by human APP overexpression in mice. *Mol Cell Neurosci* 74:34–41. <https://doi.org/10.1016/j.mcn.2016.03.004>
  41. Lu X, Kambe F, Cao X, Kozaki Y, Kaji T, Ishii T, Seo H (2008) 3beta-Hydroxysteroid-delta24 reductase is a hydrogen peroxide scavenger, protecting cells from oxidative stress-induced apoptosis. *Endocrinology* 149:3267–3273. <https://doi.org/10.1210/en.2008-0024>
  42. Lyssenko NN, Shi X, Pratico D (2022) The Alzheimer's disease GWAS risk alleles in the ABCA7 promoter and 5' region reduce ABCA7 expression. *Acta Neuropathol* 144:585–587. <https://doi.org/10.1007/s00401-022-02459-8>
  43. Mai M, Guo X, Huang Y, Zhang W, Xu Y, Zhang Y, Bai X, Wu J, Zu H (2022) DHCR24 knockdown induces tau hyperphosphorylation at Thr181, Ser199, Ser262, and Ser396 sites via activation of the lipid raft-dependent Ras/MEK/ERK signaling pathway in C8D1A astrocytes. *Mol Neurobiol* 59:5856–5873. <https://doi.org/10.1007/s12035-022-02945-w>
  44. Maiese K (2016) Targeting molecules to medicine with mTOR, autophagy and neurodegenerative disorders. *Br J Clin Pharmacol* 82:1245–1266. <https://doi.org/10.1111/bcp.12804>
  45. Malfitano AM, Marasco G, Proto MC, Laezza C, Gazerro P, Bifulco M (2014) Statins in neurological disorders: an overview and update. *Pharmacol Res* 88:74–83. <https://doi.org/10.1016/j.phrs.2014.06.007>
  46. Martin MG, Dotti CG (2022) Plasma membrane and brain dysfunction of the old: do we age from our membranes? *Front Cell Dev Biol* 10:1031007. <https://doi.org/10.3389/fcell.2022.1031007>
  47. Martin MG, Pfrieger F, Dotti CG (2014) Cholesterol in brain disease: sometimes determinant and frequently implicated. *EMBO Rep* 15:1036–1052. <https://doi.org/10.15252/embr.201439225>
  48. Martinez-Morillo E, Hansson O, Atagi Y, Bu G, Minthon L, Diamandis EP, Nielsen HM (2014) Total apolipoprotein E levels and specific isoform composition in cerebrospinal fluid and plasma from Alzheimer's disease patients and controls. *Acta Neuropathol* 127:633–643. <https://doi.org/10.1007/s00401-014-1266-2>
  49. Martiskainen H, Paldanius KMA, Natunen T, Takalo M, Marttinen M, Leskela S, Huber N, Makinen P, Bertling E, Dhungana H et al (2017) DHCR24 exerts neuroprotection upon inflammation-induced neuronal death. *J Neuroinflammation* 14:215. <https://doi.org/10.1186/s12974-017-0991-6>
  50. Mauch DH, Nagler K, Schumacher S, Goritz C, Muller EC, Otto A, Pfrieger FW (2001) CNS synaptogenesis promoted by glia-derived cholesterol. *Science* 294:1354–1357. <https://doi.org/10.1126/science.294.5545.1354>
  51. Minett T, Classey J, Matthews FE, Fahrenhold M, Taga M, Brayne C, Ince PG, Nicoll JA, Boche D, Mrc C (2016) Microglial immunophenotype in dementia with Alzheimer's pathology. *J Neuroinflammation* 13:135. <https://doi.org/10.1186/s12974-016-0601-z>
  52. Molander-Melin M, Blennow K, Bogdanovic N, Dellheden B, Mansson JE, Fredman P (2005) Structural membrane alterations in Alzheimer brains found to be associated with regional disease development; increased density of gangliosides GM1 and GM2 and loss of cholesterol in detergent-resistant membrane domains. *J Neurochem* 92:171–182. <https://doi.org/10.1111/j.1471-4159.2004.02849.x>
  53. Moll T, Marshall JNG, Soni N, Zhang S, Cooper-Knock J, Shaw PJ (2021) Membrane lipid raft homeostasis is directly linked to neurodegeneration. *Essays Biochem* 65:999–1011. <https://doi.org/10.1042/EBC20210026>
  54. Nguyen PT, Dorman LC, Pan S, Vainchtein ID, Han RT, Nakao-Inoue H, Taloma SE, Barron JJ, Molofsky AB, Kheirbek MA et al (2020) Microglial remodeling of the extracellular matrix promotes synapse plasticity. *Cell* 182:388–403 e315. <https://doi.org/10.1016/j.cell.2020.05.050>
  55. Panza F, Lozupone M, Logroscino G, Imbimbo BP (2019) A critical appraisal of amyloid-beta-targeting therapies for Alzheimer disease. *Nat Rev Neurol* 15:73–88. <https://doi.org/10.1038/s41582-018-0116-6>
  56. Papassotiropoulos A, Lutjohann D, Bagli M, Locatelli S, Jessen F, Buschfort R, Ptok U, Bjorkhem I, von Bergmann K, Heun R (2002) 24S-hydroxycholesterol in cerebrospinal fluid is elevated in early stages of dementia. *J Psychiatr Res* 36:27–32. [https://doi.org/10.1016/s0022-3956\(01\)00050-4](https://doi.org/10.1016/s0022-3956(01)00050-4)
  57. Park J, Kim H, Kim J, Cheon M (2020) A practical application of generative adversarial networks for RNA-seq analysis to predict the molecular progress of Alzheimer's disease. *PLoS Comput Biol* 16:e1008099. <https://doi.org/10.1371/journal.pcbi.1008099>
  58. Park JS, Kam TI, Lee S, Park H, Oh Y, Kwon SH, Song JJ, Kim D, Kim H, Jhaldiyal A et al (2021) Blocking microglial activation of reactive astrocytes is neuroprotective in models of Alzheimer's disease. *Acta Neuropathol Commun* 9:78. <https://doi.org/10.1186/s40478-021-01180-z>
  59. Peric A, Annaert W (2015) Early etiology of Alzheimer's disease: tipping the balance toward autophagy or endosomal dysfunction? *Acta Neuropathol* 129:363–381. <https://doi.org/10.1007/s00401-014-1379-7>
  60. Petrov AM, Kasimov MR, Zefirov AL (2016) Brain cholesterol metabolism and its defects: linkage to neurodegenerative diseases and synaptic dysfunction. *Acta Nat* 8:58–73
  61. Pfrieger FW (2003) Cholesterol homeostasis and function in neurons of the central nervous system. *Cell Mol Life Sci* 60:1158–1171. <https://doi.org/10.1007/s00018-003-3018-7>
  62. Pfrieger FW, Ungerer N (2011) Cholesterol metabolism in neurons and astrocytes. *Prog Lipid Res* 50:357–371. <https://doi.org/10.1016/j.plipres.2011.06.002>
  63. Qi Z, Zhang Y, Yao K, Zhang M, Xu Y, Zhang J, Bai X, Zu H (2021) DHCR24 knockdown lead to hyperphosphorylation of tau at Thr181, Thr231, Ser262, Ser396, and Ser422 Sites by membrane lipid-raft dependent PP2A signaling in SH-SY5Y cells. *Neurochem Res* 46:1627–1640. <https://doi.org/10.1007/s11064-021-03273-6>
  64. Rayaprolu S, Higginbotham L, Bagchi P, Watson CM, Zhang T, Levey AI, Rangaraju S, Seyfried NT (2021) Systems-based proteomics to resolve the biology of Alzheimer's disease beyond amyloid and tau. *Neuropsychopharmacology* 46:98–115. <https://doi.org/10.1038/s41386-020-00840-3>
  65. Rohanizadegan M, Sacharow S (2018) Desmosterolosis presenting with multiple congenital anomalies. *Eur J Med Genet* 61:152–156. <https://doi.org/10.1016/j.ejmg.2017.11.009>
  66. Roher AE, Weiss N, Kokjohn TA, Kuo YM, Kalback W, Anthony J, Watson D, Luehrs DC, Sue L, Walker D et al (2002) Increased A beta peptides and reduced cholesterol and myelin proteins characterize white matter degeneration in Alzheimer's disease. *Biochemistry* 41:11080–11090. <https://doi.org/10.1021/bi026173d>
  67. Sarajarvi T, Haapasalo A, Viswanathan J, Makinen P, Laitinen M, Soinen H, Hiltunen M (2009) Down-regulation of seladin-1 increases BACE1 levels and activity through enhanced GGA3 depletion during apoptosis. *J Biol Chem* 284:34433–34443. <https://doi.org/10.1074/jbc.M109.036202>
  68. Sharma VK, Singh TG, Singh S, Garg N, Dhiman S (2021) Apoptotic pathways and Alzheimer's disease: probing therapeutic potential. *Neurochem Res* 46:3103–3122. <https://doi.org/10.1007/s11064-021-03418-7>
  69. Shi Q, Chang C, Saliba A, Bhat MA (2022) Microglial mTOR activation upregulates Trem2 and enhances beta-amyloid plaque clearance in the 5XFAD Alzheimer's disease model. *J Neurosci* 42:5294–5313. <https://doi.org/10.1523/JNEUROSCI.2427-21.2022>
  70. Silingardi D, Angelucci A, De Pasquale R, Borsotti M, Squitieri G, Brambilla R, Putignano E, Pizzorusso T, Berardi N (2011) ERK pathway activation bidirectionally affects visual recognition memory and synaptic plasticity in the perirhinal cortex. *Front Behav Neurosci* 5:84. <https://doi.org/10.3389/fnbeh.2011.00084>

71. Slegers K (2020) Expression of ABCA7 in Alzheimer's disease. *Acta Neuropathol* 139:941–942. <https://doi.org/10.1007/s00401-020-02136-8>
72. Song Y, Kenworthy AK, Sanders CR (2014) Cholesterol as a co-solvent and a ligand for membrane proteins. *Protein Sci* 23:1–22. <https://doi.org/10.1002/pro.2385>
73. Sun BL, Chen Y, Fan DY, Zhu C, Zeng F, Wang YJ (2021) Critical thinking on amyloid-beta-targeted therapy: challenges and perspectives. *Sci China Life Sci* 64:926–937. <https://doi.org/10.1007/s11427-020-1810-y>
74. Thal DR, Papassotiropoulos A, Saïdo TC, Griffin WS, Mrak RE, Kolsch H, Del Tredici K, Attems J, Ghebremedhin E (2010) Capillary cerebral amyloid angiopathy identifies a distinct APOE epsilon4-associated subtype of sporadic Alzheimer's disease. *Acta Neuropathol* 120:169–183. <https://doi.org/10.1007/s00401-010-0707-9>
75. Tse KH, Herrup K (2017) Re-imagining Alzheimer's disease—the diminishing importance of amyloid and a glimpse of what lies ahead. *J Neurochem* 143:432–444. <https://doi.org/10.1111/jnc.14079>
76. Uddin MS, Kabir MT, Al Mamun A, Abdel-Daim MM, Barreto GE, Ashraf GM (2019) APOE4 and Alzheimer's disease: evidence mounts that targeting APOE4 may combat Alzheimer's pathogenesis. *Mol Neurobiol* 56:2450–2465. <https://doi.org/10.1007/s12035-018-1237-z>
77. Uddin MS, Kabir MT, Rahman MS, Behl T, Jeandet P, Ashraf GM, Najda A, Bin-Jumah MN, El-Seedi HR, Abdel-Daim MM (2020) Revisiting the amyloid cascade hypothesis: from anti-Abeta therapeutics to auspicious new ways for Alzheimer's disease. *Int J Mol Sci*. <https://doi.org/10.3390/ijms21165858>
78. Uddin MS, Stachowiak A, Mamun AA, Tzvetkov NT, Takeda S, Atanasov AG, Bergantini LB, Abdel-Daim MM, Stankiewicz AM (2018) Autophagy and Alzheimer's disease: from molecular mechanisms to therapeutic implications. *Front Aging Neurosci* 10:04. <https://doi.org/10.3389/fnagi.2018.00004>
79. Umeda T, Mori H, Zheng H, Tomiyama T (2010) Regulation of cholesterol efflux by amyloid beta secretion. *J Neurosci Res* 88:1985–1994. <https://doi.org/10.1002/jnr.22360>
80. Vance JE (2012) Dysregulation of cholesterol balance in the brain: contribution to neurodegenerative diseases. *Dis Model Mech* 5:746–755. <https://doi.org/10.1242/dmm.010124>
81. Vance JE, Hayashi H, Karten B (2005) Cholesterol homeostasis in neurons and glial cells. *Semin Cell Dev Biol* 16:193–212. <https://doi.org/10.1016/j.semcdb.2005.01.005>
82. Vorhees CV, Williams MT (2006) Morris water maze: procedures for assessing spatial and related forms of learning and memory. *Nat Protoc* 1:848–858. <https://doi.org/10.1038/nprot.2006.116>
83. Wang W, Mutka AL, Zmrzljak UP, Rozman D, Tanila H, Gylling H, Remes AM, Huttunen HJ, Ikonen E (2014) Amyloid precursor protein alpha- and beta-cleaved ectodomains exert opposing control of cholesterol homeostasis via SREBP2. *FASEB J* 28:849–860. <https://doi.org/10.1096/fj.13-239301>
84. Yadav RS, Tiwari NK (2014) Lipid integration in neurodegeneration: an overview of Alzheimer's disease. *Mol Neurobiol* 50:168–176. <https://doi.org/10.1007/s12035-014-8661-5>
85. Yao K, Wu J, Zhang J, Bo J, Hong Z, Zu H (2016) Protective effect of DHT on apoptosis induced by U18666A via PI3K/Akt signaling pathway in C6 glial cell lines. *Cell Mol Neurobiol* 36:801–809. <https://doi.org/10.1007/s10571-015-0263-x>
86. Yilmaz C, Karali K, Fodelianaki G, Gravanis A, Chavakis T, Charalampopoulos I, Alexaki VI (2019) Neurosteroids as regulators of neuroinflammation. *Front Neuroendocrinol* 55:100788. <https://doi.org/10.1016/j.yfrne.2019.100788>
87. Yin F (2022) Lipid metabolism and Alzheimer's disease: clinical evidence, mechanistic link and therapeutic promise. *FEBS J*. <https://doi.org/10.1111/febs.16344>
88. Zolotushko J, Flusser H, Markus B, Shelef I, Langer Y, Heverin M, Bjorkhem I, Sivan S, Birk OS (2011) The desmosterolosis phenotype: spasticity, microcephaly and micrognathia with agenesis of corpus callosum and loss of white matter. *Eur J Hum Genet* 19:942–946. <https://doi.org/10.1038/ejhg.2011.74>

## Publisher's Note

Springer Nature remains neutral with regard to jurisdictional claims in published maps and institutional affiliations.

Ready to submit your research? Choose BMC and benefit from:

- fast, convenient online submission
- thorough peer review by experienced researchers in your field
- rapid publication on acceptance
- support for research data, including large and complex data types
- gold Open Access which fosters wider collaboration and increased citations
- maximum visibility for your research: over 100M website views per year

At BMC, research is always in progress.

Learn more [biomedcentral.com/submissions](https://biomedcentral.com/submissions)

